Electrocatalytic oxidation of low weight oxygenated organic compounds: A review on their use as a chemical source to produce either electricity in a Direct Oxidation Fuel Cell or clean hydrogen in an electrolysis cell

Claude Lamy

▶ **To cite this version:**

Claude Lamy. Electrocatalytic oxidation of low weight oxygenated organic compounds: A review on their use as a chemical source to produce either electricity in a Direct Oxidation Fuel Cell or clean hydrogen in an electrolysis cell. Journal of Electroanalytical Chemistry, 2020, 875, pp.114426 -. 10.1016/j.jelechem.2020.114426 . hal-03493260

HAL Id: hal-03493260
https://hal.science/hal-03493260v1

Submitted on 15 Dec 2022

HAL is a multi-disciplinary open access archive for the deposit and dissemination of scientific research documents, whether they are published or not. The documents may come from teaching and research institutions in France or abroad, or from public or private research centers.

L'archive ouverte pluridisciplinaire **HAL**, est destinée au dépôt et à la diffusion de documents scientifiques de niveau recherche, publiés ou non, émanant des établissements d'enseignement et de recherche français ou étrangers, des laboratoires publics ou privés.

Distributed under a Creative Commons Attribution - NonCommercial 4.0 International License

Version of Record: https://www.sciencedirect.com/science/article/pii/S1572665720306536
Manuscript_ef0a302f326051e968e5589e1a545e29

Electrocatalytic Oxidation of Low Weight Oxygenated Organic Compounds: A Review on their Use as a Chemical Source to Produce either Electricity in a Direct Oxidation Fuel Cell or Clean Hydrogen in an Electrolysis Cell [(1)]

Claude Lamy. E-mail : claude.lamy@umontpellier.fr
Institut Européen des Membranes, Université de Montpellier, UMR CNRS 5635, 2, place Eugène Bataillon, CC 047, 34095 MONTPELLIER Cedex 5, France

[1] This article is dedicated to the memory of our close friend Andrzej Więckowski

© 2020 published by Elsevier. This manuscript is made available under the CC BY NC user license
https://creativecommons.org/licenses/by-nc/4.0/

ABSTRACT

The electrocatalytic oxidation of low weight oxygenated compounds, such as formic acid and methanol, has been the subject of many investigations since nearly fifty years both for their use in a Direct Oxidation Fuel Cell or to produce clean hydrogen by their electrochemical reforming in an Electrolysis Cell. To optimize the energy efficiency of these processes it is very important to know the reaction mechanisms of their electro-oxidation on suitable and specific electrocatalysts. Andrzej Więckowski, together with Roger Parsons, were among the major scientists involved in the determination of the reaction mechanisms of their oxidation on noble metal electrodes both by electrochemical methods (such as linear and cyclic voltammetry) and physicochemical methods, e.g. radiometry, NMR and Infrared Spectroscopy. This review paper first presents the thermodynamics and kinetics of the electrocatalytic oxidation of low weight oxygenated compounds, together with the reaction mechanisms of the electrochemical oxidation of formic acid and methanol. Then their use, as basic feedstock in a Direct Oxidation Fuel Cell for electricity production with a relatively good efficiency (≈ 40 %) or in a Proton Exchange Membrane Electrolysis Cell for the production of clean hydrogen able to feed low temperature fuel cells, is discussed.

Keywords: Electrocatalytic oxidation; Formic acid or Methanol; Reaction mechanisms; Direct oxidation fuel cells; Hydrogen generation; Electrochemical reforming.

1. Introduction

Technological civilization needs more and more energy, particularly in emerging and developing countries. Fossil resources, such as coal, natural gas and hydrocarbons, are the main primary sources, but their amount is limited and they will be exhausted in a few decades. Furthermore they are the main contribution to the emission of carbon dioxide mainly responsible for climate change. The development of clean power sources and the reduction of the emission of greenhouse gases have led to many investigations on Low Temperature Fuel Cells, such as the Proton Exchange Membrane Fuel Cell (PEMFC), fed either with pure hydrogen [1] or with other fuels, particularly low weight liquid organic compounds, such as formic acid [2, 3], methanol [4] or ethanol [5].

However the electrocatalytic oxidation of these compounds in a Direct Oxidation Fuel Cell (DOFC), such as the Direct Formic Acid Fuel Cell (DFAFC) [2, 3], the Direct Methanol Fuel Cell (DMFC) [4] or the Direct Ethanol Fuel Cell (DEFC), experiences overvoltages much larger than those encountered in a Hydrogen Fuel Cell [5].This is due to the complexity of reactions mechanisms leading to electrical performances one order of magnitude smaller than those of the hydrogen/oxygen PEMFC (e.g. $P_{max} \approx 0.35$ W cm^{-2} for the DMFC and $P_{max} \approx 0.1$ W cm^{-2} for the DEFC vs. $P_{max} \approx 1$ to 2 W cm^{-2} for the H_2/O_2PEMFC).

Thus an alternative approach is to use molecular hydrogen as an energy source and energy carrier, which strongly limits the production of greenhouse gases, depending on the primary sources used for its fabrication. With renewable energy sources, such as nuclear power, hydroelectric power, wind, solar and tidal power, the production of hydrogen by water electrolysis is the most developed process, leading to high purity hydrogen, suitable to feed low temperature Fuel Cells [1]. But due to the high overvoltages encountered in water electrolysis, particularly at the catalytic anode, where oxygen evolution does occur, the production cost is actually not competitive with the main production processes (methane steam reforming, partial oxidation, auto thermal reforming) from natural gas and hydrocarbons [6]. This is because the energy needed to produce 1 kg of hydrogen is much greater than the theoretical energy (33 kWh kg^{-1} or 3 kWh/Nm^3 under standard conditions), reaching more than 50 kWh kg^{-1} (corresponding to about 4.5 kWh/Nm^3), i.e. an energy efficiency lower than 66%.

Conversely, electrochemical reforming, consisting in the electrocatalytic oxidation of hydrogen containing compounds at the anodic side of a Proton Exchange Membrane Electrolysis Cell (PEMEC), can produce very pure gaseous hydrogen by reducing, at the cathodic side, the protons which cross-over the membrane [7]. More importantly, this process can occur under mild experimental conditions, such as ambient temperature and pressure. This is a very promising approach, since the theoretical cell voltage (around a few tens mV) for the electrolysis of these compounds is lower than the theoretical cell voltage of water electrolysis (1.23 V under standard conditions). Several organic compounds can be considered as hydrogen sources, such as carboxylic acids, alcohols, sugars, etc., e.g. formic acid [8, 9], methanol [10-12], ethanol [13, 14], glycerol [15, 16], and glucose [16]. Although the electrochemical decomposition reaction of these compounds displays a low cell voltage (under standard conditions), larger cell voltages are usually experienced under working conditions, due to the high anodic overvoltages encountered in their electrochemical oxidation.

To overcome these difficulties, which appear both in a DOFC or in a PEMEC, a right choice of suitable anode electrocatalysts is essential, namely Pd-Au electrodes for formic acid electro-oxidation [9], Pt-Ru based electrodes for methanol oxidation [17] or Pt-Sn based electrocatalysts for ethanol oxidation [5]. For methanol oxidation, Pt-Ru electrocatalysts, with a Pt to Ru atomic ratio of 1 to 1, was claimed to be the best electrocatalysts at room temperature [18], but fundamental studies, carried out in our group, shown that an atomic ratio of 4 Pt to 1 Ru led to optimized results both in a three-electrode electrochemical cell – see Fig.4 in Section 2.3– and in a elementary DMFC –see Fig.10 in Section 3.2. Thus the right choice of suitable catalysts for the electrochemical oxidation of these compounds, both in a DOFC or in a PEMEC, is based on a detailed study of the reaction mechanisms in relation with their electrocatalytic activity and their atomic structure.

In the following review paper we will first present the basic principles of the electrocatalytic oxidation of formic acid and methanol in acidic medium, whose reaction mechanisms were thoroughly investigated by Andrzej Więckowski [19]. Then electricity production by their electro-oxidation in a DOFC [20] will be discussed, and finally hydrogen production by their electrochemical reforming will be presented [21].

2. Principle of the electrocatalytic oxidation of oxygenated organic compounds

- 2.1 Thermodynamics and kinetics of the electro-oxidation reaction

A detailed knowledge of the thermodynamics and kinetics of the electrocatalytic oxidation of a given oxygenated organic compound, $C_xH_yO_z$, is essential to consider both for its use as a fuel in a Direct Oxidation Fuel Cell (DOFC), such as a PEMFC, or as a hydrogen source for clean hydrogen production in an electrolysis Cell, such as a PEMEC (Fig.1).

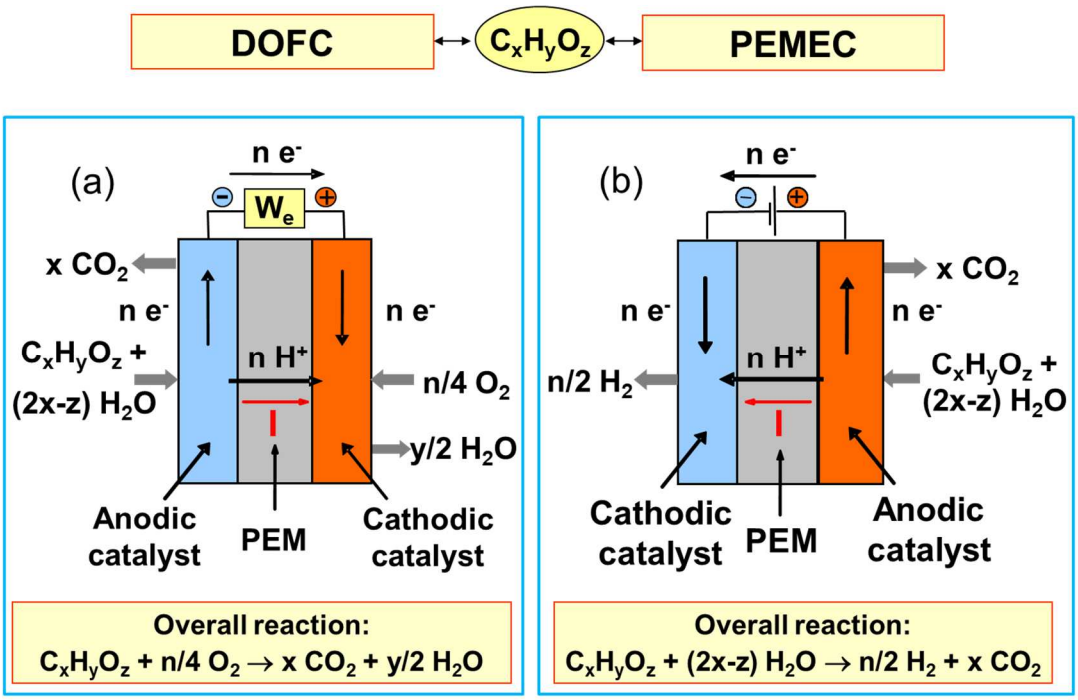

Fig.1: Schemes of a Direct Oxidation Fuel Cell (DOFC) (a) and of a Proton Exchange Membrane Electrolysis Cell (PEMEC) (b) using an oxygenated organic compound.

The complete electrocatalytic oxidation of an organic compound, $C_xH_yO_z$, in the anodic compartment of an electrochemical device working in acidic medium (fuel cell or electrolysis cell) is performed with a suitable electrocatalyst, which is specific of the considered compound, leading to carbon dioxide and protons in a complete oxidation process, according to reaction (1):

$$C_xH_yO_z + (2\,x - z)\,H_2O \rightarrow x\,CO_2 + n\,(H^+ + e^-) \qquad \text{anodic reaction} \qquad (1)$$

with n = 4x + y - 2z the number of exchanged electrons.

In the cathodic compartment of the fuel cell oxygen is reduced to water, reaction (2a):

$$O_2 + 4\,(H^+ + e^-) \rightarrow 2\,H_2O \qquad \text{cathodic reaction} \qquad (2a)$$

whereas in the cathodic compartment of the electrolysis cell the protons produced at the anode cross-over the proton exchange membrane, and are reduced to molecular hydrogen at a convenient catalyst by electrons arriving from the external circuit according to reaction (2b):

$$n\,(H^+ + e^-) \rightarrow (n/2)\,H_2 \qquad \text{cathodic reaction} \qquad (2b)$$

The electrical balance between reactions (1) and (2a) leads to the following overall reaction in a DOFC:

$$C_xH_yO_z + n/4\,O_2 \rightarrow x\,CO_2 + y/2\,H_2O \qquad \text{overall reaction} \qquad (3a)$$

corresponding to the electrochemical combustion of the organic compound in the fuel cell. On the other handthe electrical balance between reactions (1) and (2b) leads to the following overall reaction in a PEMEC:

$$C_xH_yO_z + (2\,x - z)\,H_2O \rightarrow x\,CO_2 + (n/2)\,H_2 \qquad \text{overall reaction} \qquad (3b)$$

Reaction (3b) corresponds to the electrochemical reforming of $C_xH_yO_z$ producing hydrogen and carbon dioxide by its complete oxidation in the electrolysis cell.

Knowing the thermodynamic data associated with the enthalpy of formation ΔH_i^0 and Gibbs free energy ΔG_i^0 of the compounds involved ($C_xH_yO_z$, H_2O and CO_2) one may calculate the enthalpy change and Gibbs energy change of reactions (3a) and (3b), as follows:

$$\Delta H_{FC}^0 = x\,\Delta H_{CO_2}^0 + y/2\,\Delta H_{H_2O}^0 - \Delta H_f^0 \qquad (4a)$$

$$\Delta G_{FC}^0 = x\,\Delta G_{CO_2}^0 + y/2\,\Delta G_{H_2O}^0 - \Delta G_f^0 \qquad (5a)$$

for the fuel cell reaction (3a) and:

$$\Delta H_{EC}^0 = x\,\Delta H_{CO_2}^0 - (2x - z)\,\Delta H_{H_2O}^0 - \Delta H_f^0 \qquad (4b)$$

$$\Delta G_{EC}^0 = x\,\Delta G_{CO_2}^0 - (2x - z)\,\Delta G_{H_2O}^0 - \Delta G_f^0 \qquad (5b)$$

for the electrolysis reaction (3b), where ΔH_f^0 and ΔG_f^0 are the enthalpy and Gibbs energy of formation of the organic compound $C_xH_yO_z$ under standard temperature and pressure (STP) conditions (298.15 K and 1 bar).

One may calculate the electromotive force (EMF) of the fuel cell, E_{FC}, and the cell voltage of the electrolysis cell, U_{cell}, together with the total (electric and thermal) energy needed, Δh, per mole of H_2 produced by the electrochemical decomposition of the involved compound, as follows:

$$E_{FC}^0 = -\frac{\Delta G_{FC}^0}{nF} = -(x\,\Delta G_{CO_2}^0 + y/2\,\Delta G_{H_2O}^0 - \Delta G_f^0)/nF \qquad (6a)$$

$$U^0_{cell} = + \frac{\Delta G^0_{EC}}{\mathrm{nF}} = + \left(\mathrm{x}\,\Delta G^0_{CO_2} - (2\mathrm{x} - \mathrm{z})\,\Delta G^0_{H_2O} - \Delta G^0_{\mathrm{f}}\right)/\mathrm{nF} \qquad (6b)$$

$$\Delta h^0 = \Delta H^0_{EC}/(\tfrac{\mathrm{n}}{2}) \qquad (6c)$$

The following relation between U_{cell} and E_{FC} may be derived as follows:

$$U^0_{cell} = + \frac{\Delta G^0_{EC}}{\mathrm{nF}} = + \left(\mathrm{x}\,\Delta G^0_{CO_2} - (2\mathrm{x} - \mathrm{z})\,\Delta G^0_{H_2O} - \Delta G^0_{\mathrm{f}}\right)/\mathrm{nF} = \frac{\Delta G^0_{FC}}{\mathrm{nF}} - \frac{\Delta G^0_{H_2O}}{2\mathrm{F}}$$

i.e.

$$U^0_{cell} = E^0_{H_2FC} - E^0_{FC} \qquad (6d)$$

The corresponding data for the electro-oxidation of hydrogen, formic acid and methanol under STP conditions, are given in Table 1.

Table 1: Standard thermodynamic data, cell voltage and number of hydrogen moles, N_{H_2}, produced by the electrochemical reforming of different hydrogen containing compounds.

Compound	N_{H_2} / mole	ΔG^0_{FC}/ kJ mol^{-1}	E^0_{FC} / V	ΔH^0_{EC} / kJ mol^{-1}	Δh^0 / kJ mol H_2^{-1}	ΔG^0_{EC}/ kJ mol^{-1}	U^0_{EC} / V
H_2O	1	- 237	1.23	+ 286	+ 286	+ 237	1.23
HCOOH	1	- 270	1.40	+ 31.5	+ 31.5	- 33.0	- 0.17
CH_3OH	3	- 702	1.21	+ 131	+ 44	+ 9.3	0.016

This table shows clearly that for the organic compounds considered here the theoretical total energy Δh^0 necessary to produce one mole of hydrogen by their electrochemical dissociation under standard conditions is much lower than that for water electrolysis, e.g. close to 9 times lower for HCOOH and at least 6 times lower for CH_3OH. Moreover, the theoretical electrical energy, which is proportional to the cell voltage - see eqn. (12) in Section 4 - is at least several times lower than that for water dissociation, or even negative, e.g. for HCOOH dissociation, which means that it is a spontaneous electrochemical process although the total energy ΔH^0_{EC} is positive due to a larger positive reversible heat transfer $T\Delta S$ associated with the entropy change.

However, the kinetics of the anodic reactions involved in both processes, i.e. water oxidation in the water electrolysis process or the electrocatalytic oxidation of the organic compound in the electrochemical reforming process, is relatively slow leading to high anodic overpotentials, and thus to higher cell voltages at the relatively high current density (over 1 A cm^{-2}) required for a high production rate of hydrogen (Fig. 2).

Figure 2 gives the current density, $j = I/S = \mathrm{nF}\ v/S = \mathrm{nF}\ v_i$, where I is the current intensity, S the electrode surface area, v and v_i the reaction rate and the intrinsic rate, respectively, as a function of the electrode potential $E_i(j)$ vs. the standard hydrogen electrode (SHE) taken as reference, for the different electrochemical processes involved.

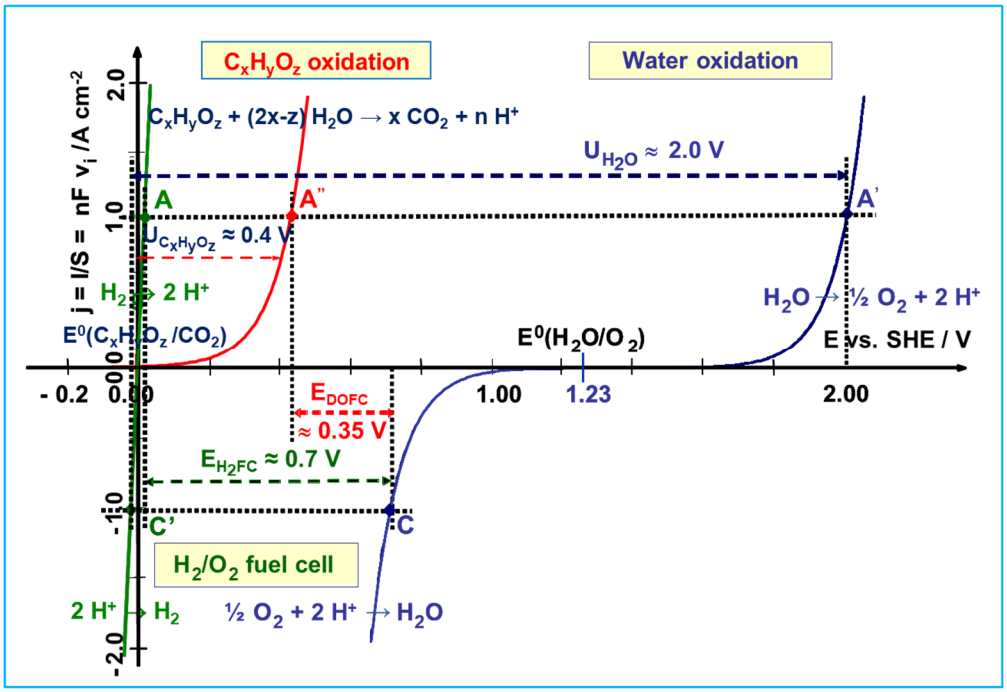

Fig.2: Theoretical electrical characteristics $j(E)$ for a reaction kinetics controlled by the Butler-Volmer law ($\alpha = 0.5$, $n = 2$): $C_xH_yO_z$ oxidation, H_2O oxidation, O_2 reduction and proton reduction. $U_{C_xH_yO_z}$, U_{H_2O}, E_{DOFC} and E_{H_2FC} are the cell voltages for $C_xH_yO_z$ electrolysis, water electrolysis, direct oxidation fuel cell and hydrogen/oxygen fuel cell at a given current density j, e.g. 1 A cm^{-2}.

When taking into account the charge transfer overpotentials η^{act}, the concentration overpotentials η^{conc} and the ohmic drop $R_e\,j$ associated with the cell resistance R_e, the cell voltage vs. current density curves, $U_{cell}(j)$, of an elementary cell, can be expressed as follows:

$$U_{cell}(j) = E_a^+(j) - E_c^-(j) + R_e|j| = U_{cell}(0) \pm (|\eta_a^{act}(j)| + |\eta_a^{conc}(j)| + |\eta_c^{act}(j)| + |\eta_c^{conc}(j)|) + R_e|j| \quad (7)$$

where the "+"sign stands for the electrolysis cell and the "-" sign for the fuel cell, respectively. In these equations $U_{cell}(0) = E_{eq}$ is the equilibrium cell voltage i.e. the cell voltage at zero current, η_i is the overpotential defined as the deviation of the electrode potential $E_i(j)$ under working conditions from its equilibrium value, i.e. $\eta_i = E_i(j) - E_{i_{eq}}(0)$, and the subscripts "a" and "c" refer to the anodic and cathodic reactions, respectively. Thus $U_{cell}(j)$ can be express as follows: $U_{cell}(j) = U_{rev}(0) \pm \eta_{loss}$, where $\eta_{loss} = \Sigma|\eta_i| + R_e|j|$ and $U_{rev}(0) = E_{eq}$.

Therefore the challenge to decrease the overvoltages, i.e. to increase the Electro-Motive Force (EMF) of the Fuel Cell E_{FC} or to decrease the cell voltage U_{cell} of the electrolyzer, is to develop new electrocatalysts able to activate the electrochemical reactions involved. These catalysts are specific of the electrochemical reactions and compounds involved.

Thus a detailed knowledge of the reaction mechanism is a key point to determine the rate determining step and to find suitable electrocatalysts able to increase the rate of this step. Many "*ex situ*" and "*in situ*" physical methods were developed for that purpose among them "in situ" radiochemical methods were early considered by Andrzej Więckowski [22] and later on NMR Spectroscopy [23] and NMR coupled to IR Reflectance Spectroscopy [24].

- 2.2 Reaction mechanisms of the electrocatalytic oxidation of Formic Acid

The electrocatalytic oxidation of formic acid, in acidic medium, has been thoroughly investigated both from a fundamental aspect [25] and for application either to the Direct Formic Acid Fuel Cell (DFAFC) [2, 3, 26] or to hydrogen production by its electrochemical reforming [8, 9].

The oxidation reaction mechanisms are very well known involving two parallel pathways for the electro-oxidation of formic acid into CO_2 [25-30], both pathways leading to the exchange of 2 electrons per formic acid molecule. For example, with Pt-based catalysts the "direct pathway" (dehydrogenation reaction), gives CO_2 directly without the formation of an adsorbed carbon monoxide species:

$$Pt + HCOOH \rightarrow Pt + CO_2 + 2\ H^+ + 2\ e^- \quad (8)$$

whereas the "indirect pathway" (dehydration reaction) involves the intermediate formation of CO, which acts as a poisoning species of Pt-based electrocatalysts, but CO can be further oxidized to CO_2 at higher potentials:

$$Pt + HCOOH \rightarrow Pt\text{-}CO + H_2O \quad (8a)$$

$$Pt + H_2O \rightarrow Pt\text{-}OH + H^+ + e^- \quad (8b)$$

$$Pt\text{-}CO + Pt\text{-}OH \rightarrow 2\ Pt + CO_2 + H^+ + e^- \quad (8c)$$

where Pt represents a platinum catalytic site.

Since the formation of OH species on Pt does occur from 0.6 V vs. the Reversible Hydrogen Electrode (RHE), the addition to Pt of a more oxidizable metal M (Ru, Mo, Mn, Sn, etc.) will enhance the rates of steps (8b) and (8c) at lower potentials, as follows :

$$M + H_2O \rightarrow M\text{-}OH + H^+ + e^- \quad (8d)$$

$$Pt\text{-}CO + M\text{-}OH \rightarrow Pt + M + CO_2 + H^+ + e^- \quad (8e)$$

Both reaction mechanisms correspond to the overall reaction:

$$Pt + HCOOH \rightarrow Pt + CO_2 + 2\ H^+ + 2\ e^- \quad (8)$$

Similar mechanisms, particularly the direct pathway, were also observed on palladium-based catalysts [31, 32], e. g. Lu et al. showed that the addition of palladium to platinum led to enhance the direct reaction pathway [31]. More recent studies have suggested that palladium and particularly palladium-based alloys have enhanced activity compared to platinum for the electro-oxidation reaction of formic acid due to the lesser formation of CO poisonous species [33-35].

In order to choose suitable anode catalysts for the electrochemical oxidation of formic acid, cyclic voltammograms were recorded in a three-electrode cell with several Pd-based electrodes in a 0.5 M H_2SO_4 solution containing 0.01 M HCOOH (Fig. 3). The presence of Pd in binary electrocatalysts allows to decrease or even to suppress the presence of CO poisoning species for pure Pd catalysts [33-35]. Thus the overvoltage of HCOOH oxidation is decreased

so that the current-density curves are shifted negatively towards low electrode potential and the overall reaction proceeds mainly through the direct pathway – see eqn.(8).

PdAu or PdPt alloys with a low content of Au or Pt (atomic ratios < 20%) display a good electrocatalytic activity, in agreement with the results obtained at low overpotentials with a PtPd catalyst in a DFAFC as shown by Rice et al. [32], and with different PdAu catalysts in a classical electrochemical cell by Zhang et al. [36]. The voltammograms of $Pd_{0.9}Au_{0.1}$/C and $Pd_{0.8}Pt_{0.2}$/C catalysts display the forward and backward sweeps remarkably quasi-superimposed (Fig. 3). This indicates that these catalytic surfaces are less sensitive to poisoning by adsorbed CO species resulting from the dissociative chemisorption of formic acid (eqn.(8a)).

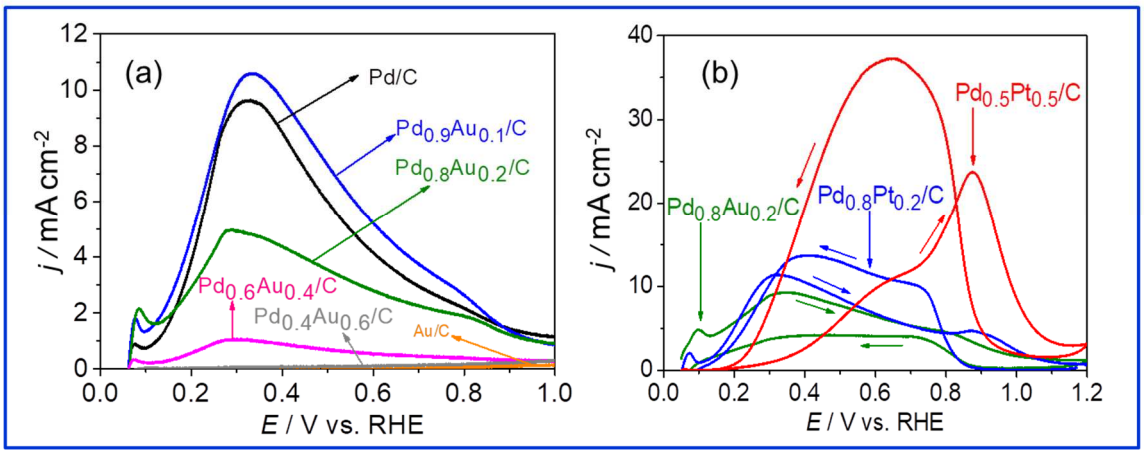

Fig. 3: Voltammetric curves recorded during the oxidation of 10^{-2} M HCOOH in 0.5 M H_2SO_4 N_2-purged electrolyte on (a) different Pd_xAu_{1-x}/C catalysts and (b) different Pd_xPt_{1-x}/C and $Pd_{0.8}Au_{0.2}$/C catalysts (T = 25 °C ; v = 50 mV s^{-1}). After [9].

The electrocatalytic behaviour of $Pd_{0.8}Pt_{0.2}$/C is particularly interesting since the oxidation of formic acid begins at electrode potentials as low as 0.1 V vs. RHE, leading to a peak current density of 12 mA cm^{-2} at 0.28 V. Similarly the $Pd_{0.9}Au_{0.1}$/C catalyst gives maximum current densities of about 11 mA cm^{-2} at 0.32 V vs. RHE.

- 2.3 Reaction mechanisms of the electrocatalytic oxidation of Methanol

The mechanism of the electro-oxidation of methanol on platinum in acidic medium was thoroughly established, mainly after the identification of both reactive intermediates and poisoning species either by electrochemical methods [37-40] or spectroscopic methods [41, 42]. The complete oxidation reaction in acid medium to reject the produced CO_2 is:

$$CH_3OH + H_2O \rightarrow CO_2 + 6\,H^+ + 6\,e^- \qquad (9)$$

In the first steps methanol is dissociatively adsorbed at Pt-based catalysts by cleavage of C-H bonds leading to the so-called formyl-like species $-(CHO)_{ads}$, according to the following steps:

$$Pt + CH_3OH \rightarrow Pt\text{-}CH_3OH_{ads} \rightarrow Pt\text{-}CHO_{ads} + 3\,H^+ + 3\,e^- \qquad (9a)$$

From this species, different steps can occur, but with platinum, the dissociation of $-(CHO)_{ads}$ gives rapidly adsorbed CO, which is responsible for the electrode poisoning. This is

the explanation of the rather poor performance of Pt catalysts, due to the relatively high potential necessary to remove such CO species by their electro-oxidation.

The kinetics of the further desorption and oxidation of $-(CHO)_{ads}$ into the reaction products is the key point of the mechanism, leading to the complete oxidation of methanol.

The usual path is the formation of CO_{ads}:

$$Pt\text{-}CHO_{ads} \rightarrow Pt\text{-}CO_{ads} + H^+ + e^- \quad (9b)$$

followed by its oxidation to CO_2 – see eqn. (9h) below, which is the rate determining step.

An alternative path to the spontaneous formation of the poisoning species (Eqn. 9b), is the oxidation of $-CHO_{ads}$ species, with OH_{ads} species coming from the dissociation of water according to the following reactions:

$$Pt + H_2O \rightarrow Pt\text{-}(OH)_{ads} + H^+ + e^- \quad (9c)$$

$$Pt\text{-}CHO_{ads} + Pt\text{-}(OH)_{ads} \rightarrow 2Pt + CO_2 + 2H^+ + 2e^- \quad (9d)$$

One parallel surface reaction, leading to adsorbed formate, has also been observed:

$$Pt\text{-}(CHO)_{ads} + Pt\text{-}(OH)_{ads} \rightarrow Pt + Pt\text{-}(COOH)_{ads} + H^+ + e^- \quad (9e)$$

then leading by further oxidation to the formation of carbon dioxide :

$$Pt\text{-}(COOH)_{ads} \rightarrow Pt + CO_2 + H^+ + e^- \quad (9f)$$

On the other hand, adsorbed CO can be oxidized through the reactions:

$$Pt\text{-}(CO)_{ads} + Pt\text{-}(OH)_{ads} \leftrightarrow Pt + Pt\text{-}(COOH)_{ads} \quad (9g)$$

followed by reaction (9f), or through the following reaction:

$$Pt\text{-}(CO)_{ads} + Pt\text{-}(OH)_{ads} \rightarrow 2Pt + CO_2 + H^+ + e^- \quad (9h)$$

This mechanism takes into account the formation of all the products as detected by Infrared Reflectance Spectroscopy (EMIRS or FTIRS) [41-44], radiochemical method [45] and liquid or gas chromatography [46]: formaldehyde through step (9a), formic acid through steps (9e) or (9g) and CO_2 through steps (9d), (9f) or (9h).

Thus, the crucial point is to determine how the $-(CHO)_{ads}$ intermediate species can be oxidized to CO_2 through various steps, as schematically summarized in Scheme 1.

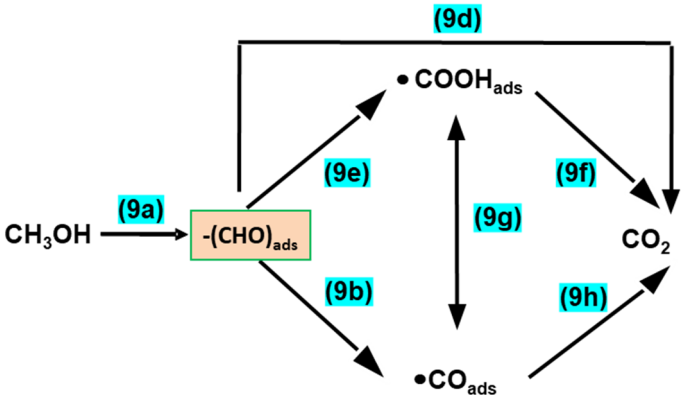

Scheme 1: Schematic representation of the mechanism of oxidation of $-CHO_{ads}$.

This scheme shows clearly that desorption and oxidation of the formyl species can follow different pathways through competitive reactions. This scheme summarizes the main problems and challenges to improve the kinetics of the electro-oxidation of methanol.

To lower the potential at which dissociation of water begins [47], a number of bimetallic and trimetallic Pt-based catalysts containing more easily oxidizable metals (Ru,

Mo, Sn, Fe, Ni, etc.) have been investigated [48-50]. With Pt-Ru catalysts, which are the best Pt-based catalysts for methanol oxidation [44, 50-53], it appears clearly from the literature, and this was fully confirmed by IR reflectance spectroscopic studies, that the presence of adsorbed -$(OH)_{ads}$ on ruthenium sites at low potentials leads to the oxidation of adsorbed CO at potentials much lower than those encountered on pure platinum. It is also probable that the -$(CHO)_{ads}$ species can be oxidized directly to carbon dioxide, without the formation of adsorbed CO poisoning species – see eqn.9d [44].

At $Pt_{1-x}Ru_x$ ($0 \le x \le 1$) electrodes the following steps of methanol oxidation can be postulated (bifunctional mechanism [54]), as follows:

• Activation of the methanol molecule by Pt:

$$Pt + CH_3OH \rightarrow Pt{-}CH_3O_{ads} + H^+ + e^- \quad (9i)$$

$$Pt{-}CH_3O_{ads} \rightarrow Pt{-}CHO_{ads} + 2\,H^+ + 2\,e^- \quad (9j)$$

$$Pt{-}CHO_{ads} \rightarrow Pt{-}CO_{ads} + H^+ + e^- \quad (9b)$$

• Activation of the water molecule either by Pt or by Ru:

$$Pt + H_2O \rightarrow Pt{-}OH_{ads} + H^+ + e^- \quad (9c)$$

$$Ru + H_2O \rightarrow Ru{-}OH_{ads} + H^+ + e^- \quad (9k)$$

• Surface reactions between the adsorbed species:

$$Pt{-}CHO_{ads} + Pt{-}OH_{ads} \rightarrow CO_2 + 2\,H^+ + 2\,e^- + 2\,Pt \quad (9d)$$

$$Pt{-}CHO_{ads} + Ru{-}OH_{ads} \rightarrow CO_2 + 2\,H^+ + 2\,e^- + Pt + Ru \quad (9l)$$

$$Pt{-}CO_{ads} + Pt{-}OH_{ads} \rightarrow CO_2 + H^+ + e^- + 2\,Pt \quad (9h)$$

$$Pt{-}CO_{ads} + Ru{-}OH_{ads} \rightarrow CO_2 + H^+ + e^- + Pt + Ru \quad (9m)$$

The activity of several bimetallic Pt-Ru electrocatalysts with different composition for methanol oxidation was recorded at room temperature as a function of the atomic composition (Fig. 4) [53].

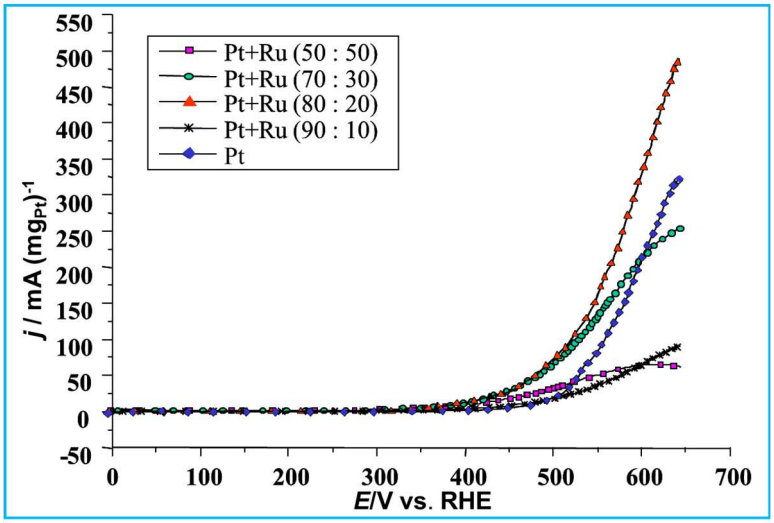

Fig.4: Current vs. potential curves for the oxidation of 0.1 M methanol in 0.5 M H_2SO_4on Pt-Ru/C electrodes as a function of their atomic composition (room temperature).After [53].

Fig.4 shows clearly that the best composition of Pt-Ru electrocatalysts is $Pt_{0.8}Ru_{0.2}$ as confirmed by recording the electromotive force and the power density vs. current density of a

DMFC using these electrocatalysts at the methanol anode (See Fig. 10 in Section 3.2). This can be interpreted by considering the number of Pt sites involved in the dissociative chemisorption of methanol leading to CO_{ads} (4 sites) vs. the number of Ru sites to dissociate water into OH_{ads} (1 site) necessary to remove CO_{ads} by its oxidation in CO_2.

3. Electricity production in a Direct Oxidation Fuel Cell

The need for power sources with greater performance than lithium batteries has increased as a result of the rapid growth of the portable electronics market, particularly the Direct Formic Acid Fuel Cell (DFAFC) and the Direct Methanol Fuel Cell (MFC) [55, 56].

- 3.1 Direct Formic Acid Fuel Cell

The DFAFC appears to be very attractive for providing higher power densities needs. With the advantages of high electromotive force, limited fuel crossover, and high practical power densities at low temperature, DFAFC are very promising power sources for portable electronics.

The electrochemical reactions involved in a DFAFC are the following:

$HCOOH \rightarrow CO_2 + 2\,H^+ + 2\,e^-$ anodic reaction with $E^0a = -0.17$ V vs. SHE (8)

$½\,O_2 + 2\,H^+ + 2\,e^- \rightarrow H_2O$ cathodic reaction with $E^0_c = 1.23$ V vs. SHE (2a)

$HCOOH + ½\,O_2 \rightarrow CO_2 + H_2O$ overall reaction with $E^0 = E^0_c - E^0a = 1.40$V (3c)

Formic acid exhibits a smaller crossover through Nafion® membrane than methanol [57, 58], allowing the use of highly concentrated fuel solutions and thinner membranes in DFAFCs. DFAFCs also have an electromotive force (EMF), as calculated from the Gibbs free energychange (see Table 1 in Section 2.1), which is higher than that of either hydrogen or direct methanol fuel cells.

The theoretical energy efficiency under standard reversible conditions is given by:

$$\varepsilon_{rev} = \frac{\Delta G^0}{\Delta H^0} = \frac{270}{254} = 1.063 \approx 106\,\% \quad (10a)$$

which is higher than unity since the entropic heat ($\Delta Q_{rev} = T\Delta S > 0$) is directly transferred to the cell. Under usual operating conditions at a cell voltage E(j) = 0.5 V, the energy efficiency will be come:$\varepsilon_{cell} = \varepsilon_{rev} \times \varepsilon_E = 1.063 \times (0.5 / 1.4) = 0.379 \approx 38\%$, where $\varepsilon_E = E(j) / E^0 = 0.5 / 1.4 = 0.357$ is the voltage efficiency.

The major disadvantage of formic acid as a fuel is its volumetric energy density, which is only 2.00 kWh $(dm^3)^{-1}$, i.e. much lower than that of methanol (6.1 kWh kg^{-1} or 4.82 kWh $(dm^3)^{-1}$. However, this disadvantage can be compensated by using higher concentrations of formic acid (Fig.5).

Fig. 5A shows the effect of formic acid concentration on the cell polarization curves. There is a relatively small reactivity of 2 M formic acid solution. The cell activity increases with feed concentration until 15 M beyond which the entire cell polarization curve profile drops greatly. At fuel feed concentrations at and below 10 M, there is a mass transport limitation in the supply of formic acid to the anode, as seen by the limiting current at lower cell voltages. A key feature is the relatively high Open Circuit Voltage (OCV) of the cell, i.e.

0.72 V. Fig.5B shows that the power density vs. current density plot goes through a maximum of 50 mW cm^{-2} at a concentration of around 12 M HCOOH.

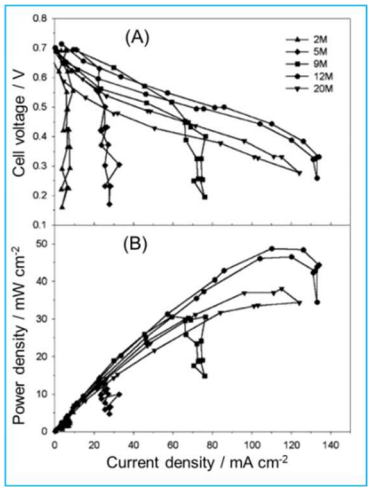

Fig.5:Cell voltage (A) and power density (B) vs. plots of formic acid oxidation with a Membrane Electrode Assembly (MEA) consisting of a Nafion®117 membrane coated with unsupported platinum black (Johnson Matthey,7 mg/cm^2 at the cathode and 4 mg/cm^2 at the anode) for different HCOOH concentrations at 60 °C. After [2].

The effect of HCOOH concentration (between 1 and 22 M) on the current density at 0.4 V is plotted in Fig.6, showing a maximum current density of 120 mA cm^{-2} for 15 M.

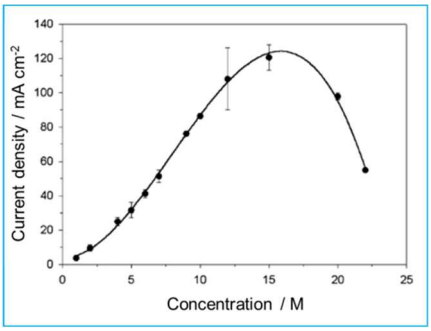

Fig.6: Plot of the current density at a 0.4 V cell voltage vs. formic acid concentration. Cell temperature 60°C; formic acid flow rate 1 ml/min. Humidified (70°C) O_2 supplied at a flow rate of 100 sccm. After[2].

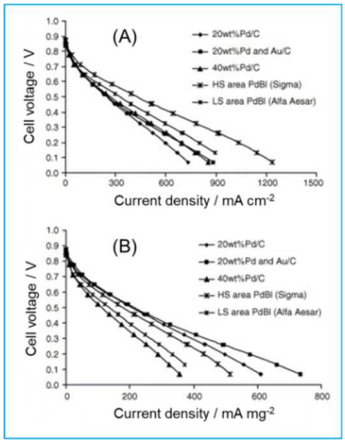

Fig. 7:Cell voltage vs. current density curves on a per membrane surface area basis (A) and a per total catalyst weight basis (B) of a direct formic acid fuel cell with various Pd anode catalysts operating in dry air at 30°C with 5 M HCOOH. After [33].

Fig. 7(A and B) shows the performance of different Pd-based anode catalysts in a real fuel cell calculated on either a geometrical active surface area basis or on a Pd weight basis.

The Sigma-Alrich Pd black gives the best overall performance, whereas the 20 wt% PdAu on carbon and the 40 wt.% Pd on carbon display similar performance and the 20 wt.% Pd/C performs slightly lower than the other two carbon-supported catalysts[33].

Figs. 8(A) and (B) give the corresponding power density vs. current density plots. The high surface area Sigma-Aldrich Pd black shows the highest maximum power density of 260 mW cm^{-2} and is able to provide this at the highest current density of all the catalysts on a geometrical active surface area basis. Fig. 8(B) shows that the 20 wt. % PdAu catalyst is the most efficient with a power density of 135 mW mg^{-1} at the highest current density on a Pd catalyst weight basis.

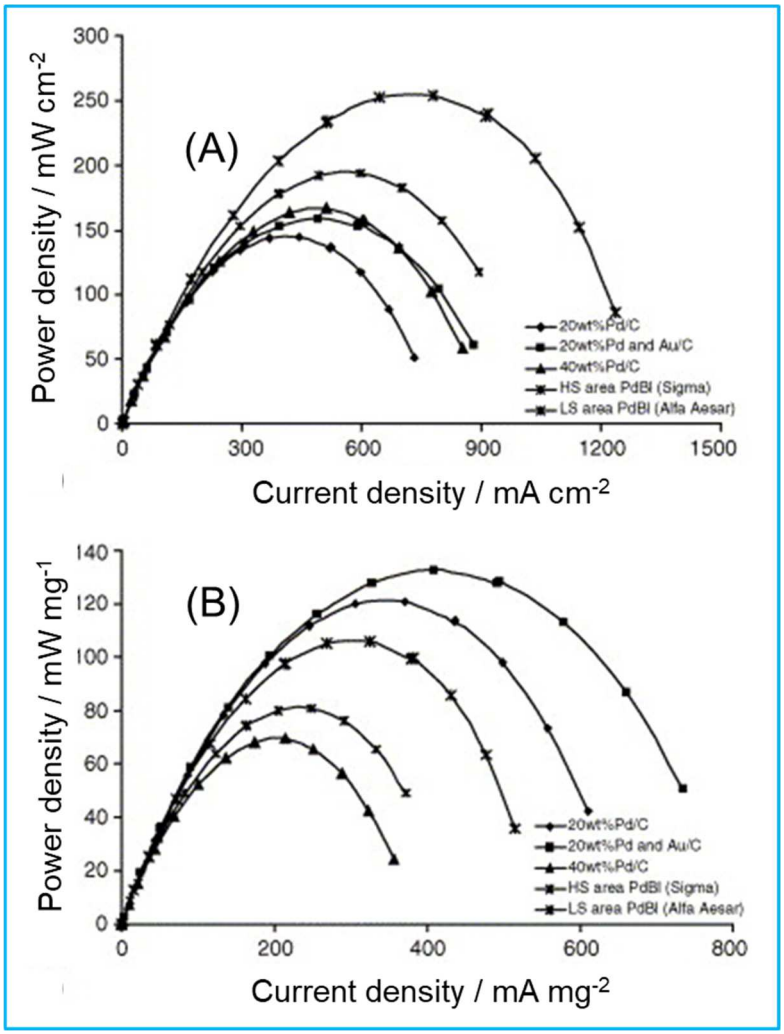

Fig. 8: Power density vs. current density plots on a per membrane surface area basis (A) and a per total catalyst weight basis (B) of a direct formic acid fuel cell with various Pd anode catalysts operating in dry air at 30°C with 5 M formic acid. After [33].

Palladium-based electrocatalysts have been confirmed to be the most efficient ones for the DFAFC since they prevent the formation of adsorbed CO poisonous species as encountered with Pt catalysts [56].

- 3.2 Direct Methanol Fuel Cell

The electrocatalytic oxidation of methanol has gained much interest over a number of years because it is the simplest alcohol which can be completely oxidized to carbon dioxide in a Direct Methanol Fuel Cell [18, 59, 60], thus providing the maximum energy densities (6.09 kWh kg^{-1} or 4.82 kWh dm^{-3}) by its complete electro-oxidation [46}. The great advantage of a DMFC is that methanol is a liquid fuel, thus more easily handled and stored than hydrogen. Methanol is produced in great quantity from natural gas (NG) by steam methane reforming (SMR) at a relatively low cost (~ 0.2 US$ l^{-1}). The development of Proton Exchange Membrane (PEM) led to a great simplification of the fuel cell by developing a DOFC avoiding the use of a reformate gas with a low concentration of CO (< 10 ppm, otherwise it may strongly poison the platinum-based electrode catalysts used). Due to system simplicity, DMFCs are particularly efficient power sources for portable electronics (cell phones, laptop computers, cam recorders, etc.) and for small size applications (micro power sources, power sources for the soldier, propulsion of small devices, e.g. golf carts, drones, etc.).

A DMFC consists of two electrodes, a catalytic methanol anode, and a catalytic oxygen cathode, separated by an ionic conductor, preferably an acid electrolyte, such as a PEM, for rejecting the carbon dioxide produced. Great progress was recently made by feeding methanol directly to the anodic compartment of a Proton Exchange Membrane Fuel Cell (PEMFC), in which the protonic membrane, e.g. Nafion®, plays both the role of an acidic electrolyte and of a separator between the two electrode compartments (Fig. 9). This technology has the added advantage of thin elementary cells and hence of compact stacks.

The electrochemical oxidation of methanol occurs on the anode electrocatalyst (e.g. dispersed platinum-based catalysts), which constitutes the negative pole of the cell:

$$CH_3OH + H_2O \rightarrow CO_2 + 6H^+ + 6\,e^- \quad \text{anodic reaction with } E^0a = 0.016 \text{ V vs. SHE} \qquad (9)$$

whereas the electrochemical reduction of oxygen occurs at the cathode (also containing a platinum based catalyst) which constitutes the positive pole of the cell :

$$O_2 + 4H^+ + 4e^- \rightarrow 2\,H_2O \quad \text{cathodic reaction with } E^0c = 1.23 \text{ V vs. SHE} \qquad (2a)$$

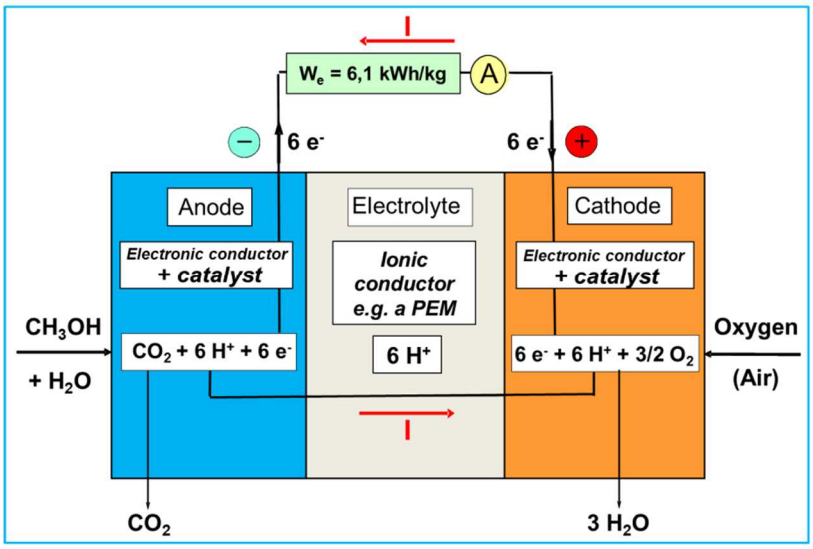

Fig.9: Schematic diagram of a DMFC based on a Proton Exchange Membrane.

leading to the overall chemical reaction:

$CH_3OH + 3/2\ O_2 \rightarrow CO_2 + 2\ H_2O$ overall reaction with $E^0 = E^0_c - E^0a = 1.21$ V (3d)

The thermodynamic data and reaction mechanisms were previously discussed (see Sections 2.1 and 2.3)

The main features of the DMFC are its high specific energy (W_s) and high volume energy density (W_{el}), the values of which are calculated as follows:

$$W_s = \frac{(-\Delta G^0)}{3600 \mathrm{x} M} = \frac{702 \mathrm{x} 10^3}{3600 \mathrm{x} 0.032} = 6.09 \approx 6.1\ \mathrm{kWhrkg^{-1}} \qquad (11)$$

and $W_{el} = W_s \times \rho = 4.82$ kWhr dm^{-3}, where M = 0.032 kg is the molar weight of methanol and $\rho = 0.7914$ kg dm^{-3} its density.

Under standard reversible conditions (25°C), the theoretical energy efficiency is very high:

$$\varepsilon_{rev} = \frac{W_e}{(-\Delta H^0)} = \frac{\mathrm{nF}E^0}{(-\Delta H^0)} = \frac{\Delta G^0}{\Delta H^0} = \frac{702}{726} = 96.7\ \% \qquad (10b)$$

It is considerably higher than that of a H_2/O_2 fuel cell (i.e. 83 %).

However under usual operating conditions, at a current density j, the electrode potentials deviate from their equilibrium values due to large overpotentials, η_i, at both electrodes and an additional loss due to the cell resistance R_e (arising mainly from the proton conducting membrane). Thus the energy efficiency will be decreased proportionally to the so-called voltage efficiency:

$$\varepsilon_E = E(j)/E^0$$

where E(j) is the cell voltage under working conditions.

For a DMFC working at 200 mA cm^{-2} and 0.5 V (e.g. with a Pt-Ru anode), this ratio will be:

$$\varepsilon_E = 0.5/1.21 = 41.3\ \%$$

and the overall efficiency of the fuel cell will be:

$$\varepsilon_{cell} = \varepsilon_{rev} \times \varepsilon_E = 0.967 \times 0.413 \approx 40\%$$

assuming a Coulombic efficiency of 100 %, i.e. the total combustion of methanol to CO_2.

The electrical characteristic of a DMFC depends strongly on the nature and structure of the anode catalysts. Pt-Ru nanoparticle catalysts dispersed on an electron conductive substrate, such as a Vulcan XC-72R carbon powder, have been recognized to give the best results, because Ru is able to suppress poisoning effect on Pt by surface oxidation of the strongly adsorbed CO, as confirmed recently [61].

The bimetallic composition is particularly important and the optimum atomic composition was found to be 20% Ru *vs.* 80% Pt, i.e. an atomic ratio Pt:Ru close to 4:1, as illustrated in Figure 10 [62].

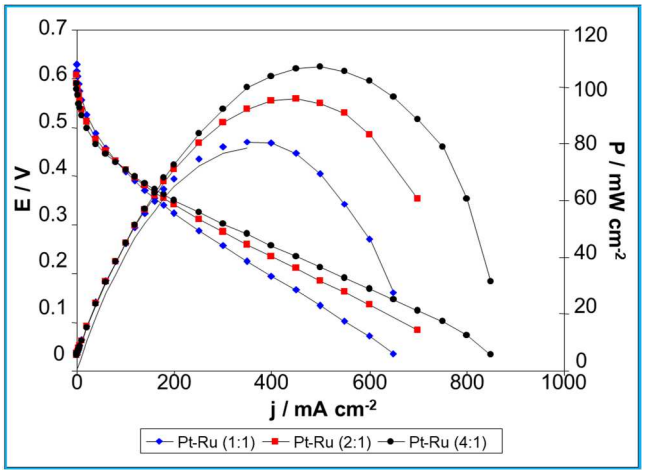

Fig.10: $E(j)$ and $P(j)$ curves of a single DMFC with Pt-Ru/C electrodes of different Pt-Ru atomic ratios. Anode loading: 2 mg cm^{-2} Pt-Ru / C; Membrane: Nafion® 117; Cathode loading: 2 mg cm^{-2} Pt/C; [MeOH] = 2 M, 2 mL min^{-1}, p_{MeOH} = 2 bar; T_{cell} = 110°C; O_2 = 120 mL min^{-1}, p_{O2} = 2.5 bar; $T_{MeOH} = T_{O2}$ = 95°C. After Ref. [62].

4. Hydrogen production by the electrochemical decomposition of low weight oxygenated organic compounds

Instead of water several organic compounds, such as carboxylic acids, e.g. formic acid, or low weight alcohols, e.g. methanol, ethanol, have been considered as convenient sources for the production of clean hydrogen by their electrocatalytic oxidation in a PEMEC. This is a very challenging approach since the cell voltage $U_{cell}(j)$) under working conditions (e.g j ≈ 1 A cm^{-2}) is of the order of 0.5-1.0 V, which is much smaller than that of water electrolysis (1.6 to 2.0 V).

Thus the electrical energy used will be at least 2 to 4 times smaller than that of water splitting according to the following relation giving the energy consumed to produce 1 Nm^3 of hydrogen [63], which is directly proportional to $U_{cell}(j)$, according to equation (12):

$$W_e(\text{in kWh/Nm}^3) = \frac{\tilde{n}F}{3600\, V_{mol} \times 10^3} U_{cell}(j) = 2.191\, U_{cell}(j) \approx 2.2\, U_{cell}(j) \qquad (12)$$

where ñ = 2 is the number of Faraday per mole of hydrogen produced and V_{mol} = 24.465 10^{-3} m^3 mol^{-1} is the molar volume of an ideal gas at a temperature of 25°C under a pressure of 1 atm., i.e. 101.325 kPa (normal conditions for gaseous species).

On the other hand, the rate of hydrogen produced can be evaluated by measuring the volume of evolved hydrogen, V_{H2}, which is a linear function of electrolysis time Δt and current intensity I, i.e. of the quantity of electricity involved $\Delta q = I\,\Delta t$, as derived from the Faraday's law, giving the rate of hydrogen evolution [63]:

$$dV_{H2}/dt = V_{mol}\,(dN_{H2}/dt) = V_{mol}\,(I/\,\tilde{n}\,F) \qquad (13)$$

$$dV_{H2}/dt = V_{mol}\,(I/2F) \times 60 = 7.607\, I \text{ (in cm}^3\text{ min}^{-1}\text{)} \qquad (13a)$$

where N_{H2} is the number of hydrogen mole, F = 96485 C per mole of electron is the Faraday constant and I is the current intensity.

The quantity of hydrogen produced after a given electrolysis time (e.g. Δt = 15 min) at a given temperature, when a quasi-stationary state is reached, can be obtained by integration of equation (13), i.e.:

$V_{H2} = V_{mol}\ (I\Delta t/2F) = 24.465\ 10^{-3} I\ (60 \times 15)/(2 \times 96485) = 114.1 \times I$ (in cm^3) at 25°C (13b)

or $V_{H2} = 119.8 \times I\ cm^3$ at 40°C and $V_{H2} = 131.3 \times I\ cm^3$ at 70°C (13c)

taking into account the hydrogen molar volume at 40°C or 70°C (dilatation of an ideal gas).

The energy efficiency ε_{cell} of an electrolysis cell can be defined as the ratio between the theoretical amount of total energy W_t (at j = 0) = ΔH_{EC} required to decompose the organic compound $C_xH_yO_z$ with the production of (n/2 = 2x+y/2-z) moles of hydrogen, according to the overall equation (3b), and the real amount of energy W_r (at j ≠ 0) used [64], i.e.:

$$\varepsilon_{EC} = \frac{W_t(j=0)}{W_r(j\neq 0)} = \frac{\Delta H_{EC}\ (j=0)}{\Delta H_{EC}(j\neq 0)} = \frac{\Delta H_{EC}\ (j=0)}{\Delta H_{EC}(j\neq 0) + nF\ \eta_{loss}} \quad (14)$$

with $W_r = \Delta H_{EC} + nF\eta_{loss}$ where $\eta_{loss} = \Sigma|\eta_i| + R_e|I| = U_{cell} - U_{rev}$ represents the energy losses due to internal dissipation via the charge transfer overvoltages $\Sigma|\eta_i|$ and the ohmic drop R_eI.

First of all the oxidation of formic acid, which is easily catalytically decomposed into hydrogen and carbon dioxide, is presented as a convincing proof of concept. Then the example of methanol for its great industrial interest will be given since it is produced at a low cost from natural gas. Furthermore it can be completely decomposed into hydrogen and carbon dioxide, so that it is an excellent liquid storage of hydrogen.

- 4.1 Electrochemical decomposition of Formic Acid

For producing hydrogen by electrochemical reforming, formic acid is fed to the anodic compartment of a PEMEC, where its oxidation produces carbon dioxide and protons, i.e.:

$$HCOOH \rightarrow CO_2 + 2\ H^+ + 2\ e^- \quad (8)$$

Then the protons cross-over the protonic membrane and reach the cathodic compartment, where they are reduced to hydrogen according to reaction (2b).

This corresponds to the electrochemical reforming of formic acid into hydrogen and carbon dioxide, according to the overall reaction:

$$HCOOH \rightarrow H_2 + CO_2 \quad (15)$$

This decomposition reaction need external energy ($\Delta H^{+0} > 0$ - see Table 1 in Section 2.1), coming from the external electrical power source and of the surrounding heat, but in the case of formic acid the decomposition is spontaneous, since $\Delta G^{+0} < 0$. The corresponding theoretical cell voltage, under standard conditions, can be calculated from ΔG^{+0}, i.e. $U^0_{cell} = (\Delta G^{+0} - \Delta G^{-o})/2F = E_a^+ - E_c^- \approx E_a^+$ because $E_c^0 \approx 0$ for the cathode in contact with evolving hydrogen under atmospheric pressure, so that $U^0_{cell} \approx \Delta G^{+0}/2F = -33\ 10^3 / 2F \approx -0.17$ V. Thus assuming that some extra thermal energy is transferred from the surrounding (whose temperature can be controlled by a thermostat or a heat exchanger) to the electrolysis cell through the reversible heat transfer $\Delta Q_{rev} = T\Delta S$, the decomposition reaction of formic acid is a spontaneous process.

However the relatively slow kinetics of the anodic reaction leads to high anodic overpotentials at high current densities (over 1 A cm^{-2}) necessary for high hydrogen

production rates, i.e. relatively high cell voltages leading to high electrical energy consumption – see eqn. (12). In order to reduce the cell voltage to acceptable values (e.g. U_{cell} < 0.9 V corresponding to an electrical energy used W_e < 1.0 kWh $(Nm^3)^{-1}$ – see Table 2-, new electrocatalysts have been developed, such as Pt-based catalysts [32] or Pd-based catalysts which have been recognized to be very active for the electrocatalytic oxidation of formic acid [9, 31, 33-35].

In order to choose the most suitable anode catalysts for the electro-oxidation of formic acid, cyclic voltammograms were recorded in a three-electrode cell with several Pd-based electrodes in a 0.5 M H_2SO_4 solution containing 0.01 M HCOOH (see Fig.3 in Section 2.2).

Therefore long-term electrolyses of formic acid were carried out at a constant controlled current intensity (0.2 to 1 A, e.g. a current density from 40 to 200 mA $cm^{-2}$for a 5 cm^2 surface area electrolysis cell) with several Pd-based electrocatalysts ($Pd_{0.8}Au_{0.2}$/C, $Pd_{0.9}Au_{0.1}$/C and $Pd_{0.8}Pt_{0.2}$/C). The cell voltage, U_{cell} at a fixed current intensity, was recorded as a function of time (Fig.11a) and of the current density after 30 min electrolysis for the oxidation at 25°C of (2 M, 5 M and 10 M) formic acid (Fig.11b).

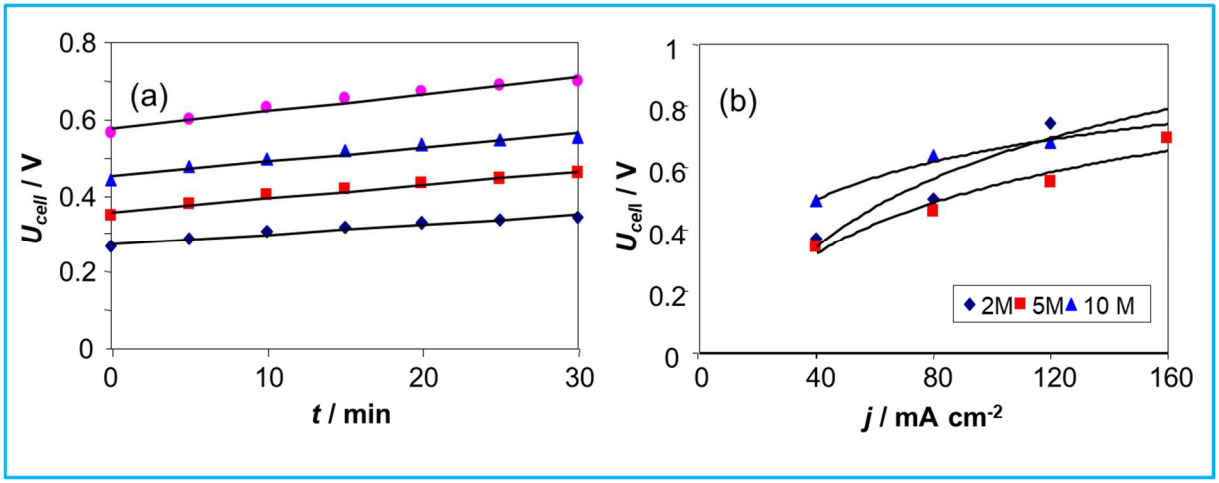

Fig 11: Electrolysis cell voltage U_{cell} (a) vs. electrolysis time at different current density j - (♦) j = 40 mA cm^{-2}, (■) j = 80 mA cm^{-2}, (▲) j = 120 mA cm^{-2}, (●) j = 160 mA cm^{-2} - and (b) vs. current density after 30 min electrolysis for the oxidation at 25°C of (2 M, 5 M and 10 M) formic acid in a PEMEC (0.5 M H_2SO_4, Pt/C, N117, $Pd_{0.8}Au_{0.2}$/C).

In all experiments the measured volume of hydrogen is a linear function of time (Fig 12) and of the current intensity I (Fig. 13), according to eqn. (13b). Figure 13 summarizes all the results obtained with the 3 electrocatalysts ($Pd_{0.8}Au_{0.2}$/C, $Pd_{0.9}Au_{0.1}$/C and $Pd_{0.8}Pt_{0.2}$/C) investigated. This shows clearly that the volume of evolved hydrogen does not depend on HCOOH concentration, or on the nature of the electrode catalyst.

The experimental results, $V_{H_2}(30')$ for 30 min electrolysis, are compared to the theoretical values calculated from the Faraday law –see eqn. (13b)–,showing a very good agreement in all experiments, but with experimental values slightly higher, which may come from the room temperature a little bit higher than 25 °C. This positive deviation in the measured volume of evolved hydrogen could also be due to resistive heating in the cell during long term electrolysis leading to an increase of the temperature of the exhaust gas [9].

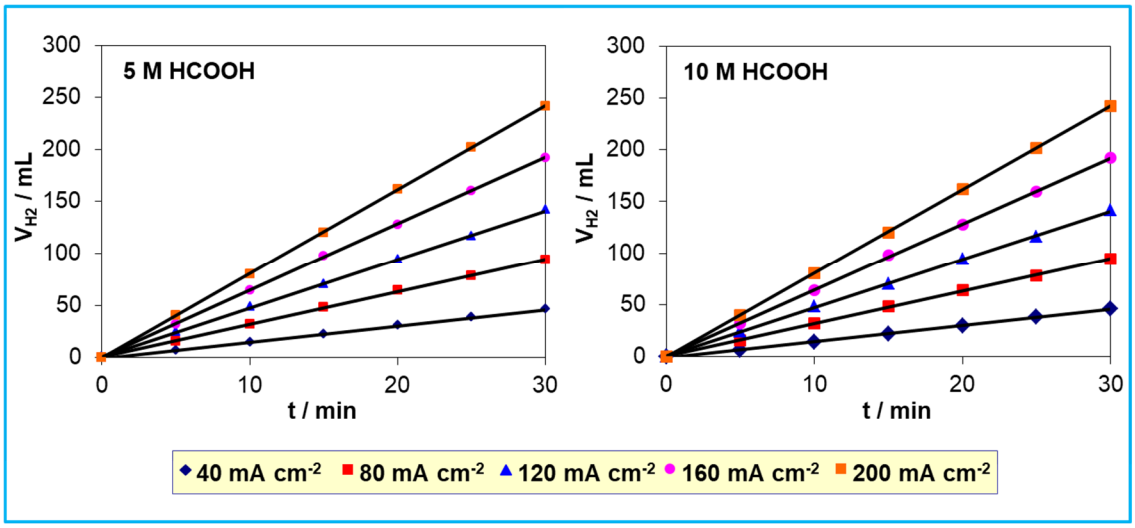

Fig. 12: Hydrogen evolution vs. electrolysis time at several current densities for the PEMEC (0.5 M H_2SO_4, Pt/C, N117, $Pd_{0.8}Au_{0.2}$/C, 5 and 10 M HCOOH) at 25 °C. (♦) j = 40 mA cm^{-2}, (■) j = 80 mA cm^{-2}, (▲) j = 120 mA cm^{-2}, (●) j = 160 mA cm^{-2}, (■) j = 200 mA cm^{-2}.

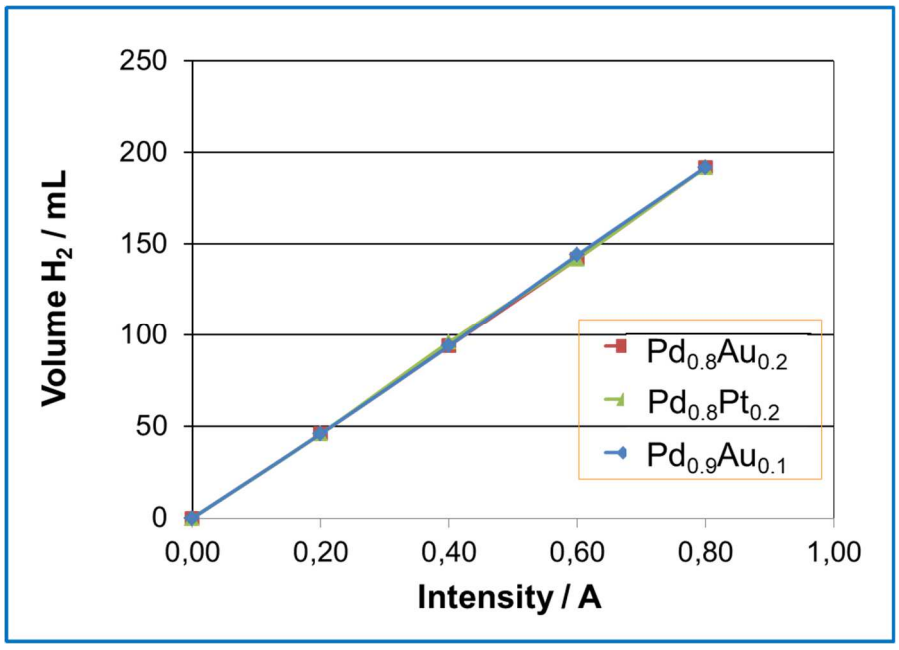

Fig. 13: Hydrogen evolution at 25 °C as a function of the current intensity for the PEMEC with different anode catalyst (0.5 M H_2SO_4, Pt/C, N117, Pd_xM_{1-x}/C) and several HCOOH concentrations (2 to 10 M); (■) $Pd_{0.8}Au_{0.2}$/C, (▲) $Pd_{0.8}Pt_{0.2}$/C, (◆) $Pd_{0.9}Au_{0.1}$/C.

For all experiments the electrical energy needed to produce one Nm^3 of hydrogen was also evaluated, since it is only a function of the cell voltage U_{cell}, according to equation (12).

Table 2 summarizes the results obtained for a $Pd_{0.8}Au_{0.2}$/C catalyst at 25°C with [HCOOH] = 5 M, giving the measured cell voltage, U_{cell}, and the electrical energy needed, W_e, both at the beginning of the electrolysis experiment and after 30 min electrolysis.

Table 2: Summary of the results obtained for $Pd_{0.8}Au_{0.2}$/C at 25 °C with [HCOOH] = 5 M; U_{cell} is the PEMEC voltage and W_e is the electrical energy.

I / A	$U_{cell(t=0)}$ / V	$W_{e_{(t=0)}}$ / kWh $(Nm^3)^{-1}$	$U_{cell(t=30')}$ / V	$W_{e_{(t=30')}}$ / kWh $(Nm^3)^{-1}$
0.2	0.231	0.51	0.295	0.65
0.4	0.312	0.68	0.370	0.81
0.6	0.327	0.72	0.384	0.84
0.8	0.468	1.03	0.531	1.16
1.0	0.633	1.39	0.806	1.77

In all the results obtained the amount of electrical energy is below 1.8 kWh $(Nm^3)^{-1}$ (for U_{cell} < 0.8 V, i.e. I <1 A), which is at least 2 to 3 times lower than the energy consumed in water electrolysis.

The energy efficiency coefficient of an electrolysis cell fed with 5 M HCOOH at 25°C working at I = 600 mA and at a cell voltage U_{cell} = 0.384 V leading to an energy loss $nF\eta_{loss}$ = nF (U_{cell} - U_{rev}) = 2x96.485 (0.384-(-0.17)) = 106.9 kJ $mole^{-1}$and a decomposition reaction enthalpy ΔH_{EC} = 31.5 kJ (see Table 2) would be:

$$\varepsilon_{EC} = \frac{\Delta H_{EC}}{\Delta H_{EC} + nF\ \eta_{loss}} = \frac{31.5}{31.5 + 106.9} = 0.228 \approx 23\ \%$$

- 4.2 Electrochemical decomposition of Methanol

Most of the previous studies on the electrochemical decomposition of methanol concerned the production of pure hydrogen by electrolysis [10, 11, 65-67] focusing on the effect of MeOH concentration (1 to 18 M) and temperature (30 to 90 °C) on the rate of hydrogen evolution. None of these studies, except the work of Cloutier and Wilkinson [12] and that of Sapountzi et al. [68], by introducing a reference electrode in a dual-chamber electrolysis cell, did investigate the kinetics of methanol oxidation under electrolysis conditions. If most of these studies used a Nafion® 117 membrane, a Pt-Ru anode and a Pt cathode to realize the Membrane-Electrode Assembly (MEA), they did not correlate clearly the hydrogen evolution rate with the current intensity flowing through the electrolysis cell as well as with the methanol concentration and cell temperature.

The principle of the electrochemical decomposition of methanol in a PEMEC involves its electrocatalytic oxidation similarly to what occurs at the anode of a DMFC [17]. In the anodic compartment, i.e. the positive pole of the electrolysis cell, methanol is oxidized on the Pt-Ru catalyst, producing carbon dioxide and protons, according to reaction (9):

$$CH_3OH + H_2O \rightarrow CO_2 + 6\ H^+ + 6\ e^- \qquad \text{anodic reaction} \qquad (9)$$

Then the protons, after crossing-over the protonic membrane, reach the cathodic compartment, i.e. the negative pole of the electrolysis cell, where they are reduced to molecular hydrogen according to reaction (2b) – see Section 2:

This corresponds to the overall electrochemical decomposition of methanol into hydrogen and carbon dioxide, according to reaction (16):

$$CH_3OH + H_2O \rightarrow CO_2 + 3\ H_2 \qquad (16)$$

This reaction is similar to methanol steam reforming, but it can occur at room temperature instead of elevated temperatures (200 to 400 °C) for methanol reforming [69, 70].

Before proceeding the electrochemical reforming of methanol it is important to know the behavior of Pt-Ru catalysts which were recognized to be the most active electrocatalysts for methanol oxidation since the addition of Ru to Pt allows the removal of the poisoning intermediate by its oxidation at lower potentials (Section 2.3). This can be done by recording CO stripping voltammograms (Fig. 14) of both pristine CO and adsorbed CO from methanol decomposition [71].

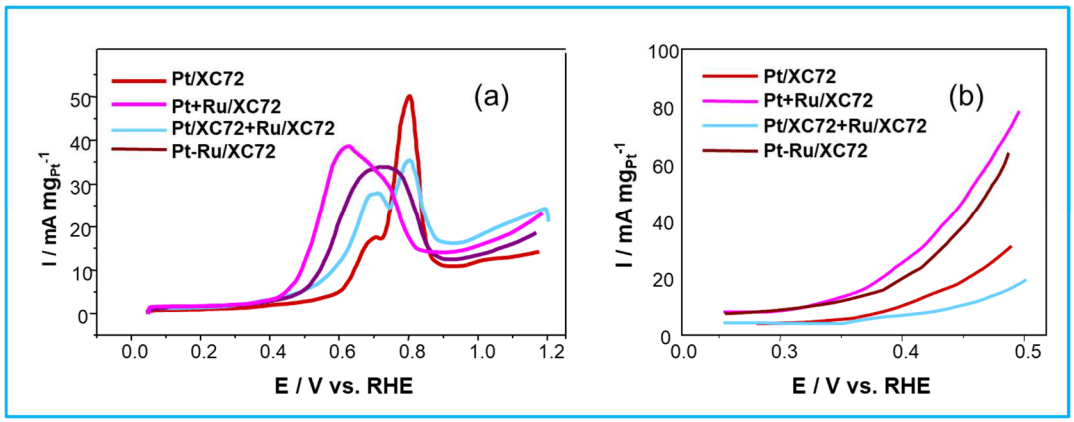

Fig. 14: CO stripping voltammograms (25°C, 10 mV s^{-1}, 0.1 M $HClO_4$) of the supported catalysts: Pt/XC72 (.—.); Pt-Ru(80:20)/XC72 (.▬.); Pt+Ru(80:20)/XC72 (.▬.); Pt/XC72+Ru/XC72 (.▬.); CO adsorption from (a) a CO saturated solution at 0.1 V for 3 min.; (b) a 0.1 M methanol solution. After [71].

Quasi-stationary polarization curves were recorded at a sweep rate of 1 mV s^{-1} and several temperatures (25 to 85 °C) in a PEMEC, consisting of a DMFC Hardware with a Pt/C negative electrode and a Pt-Ru (1/1 atomic ratio)/C positive electrode of 5 cm^2 surface area separated by a Nafion 117 membrane, fed with 1 M methanol added to the supporting electrolyte (0.5 M H_2SO_4). These curves are shown in Fig. 15 for a cathodic limit of 0.2 V vs. RHE and an anodic limit of 0.8 V in order to prevent Ru dissolution from the Pt-Ru anode. The general shape of these curves is similar to that of the voltammograms recorded in a three-electrode electrochemical cell for a Pt-Ru dispersed electrode [53].

The electrolysis was performed in a Direct Methanol Fuel Cell (DMFC) hardware used as a Proton Exchange Membrane Electrolysis Cell (PEMEC) [63]. The Pt/C hydrogen electrode of the DMFC served as a reference electrode, so that it was possible to analyze the kinetics of methanol oxidation at a catalytic Pt-Ru/C anode with the data extracted from the cell voltage vs. current intensity corrected from ohmic losses.

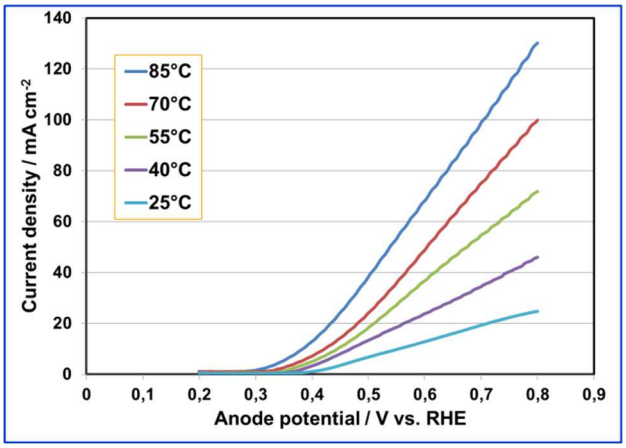

Fig. 15: Quasi-stationary polarization curves recorded at 1 mV s^{-1} and at several temperatures (from 25°C to 85 °C) for the oxidation of 1 M methanol in 0.5 M H_2SO_4 in a DMFC of 5 cm^2 surface area electrodes with a PtRu(1:1)/C anode (4 mg cm^{-2}).

Electrolyses of several methanol solutions with concentrations ranging from 0.1 M to 10 M were carried out in the DMFC hardware at different temperatures from 25 °C to 85 °C and at several constant controlled current densities from j = 1 to 100 mA cm^{-2}. In each case the cell voltage U_{cell} and the volume of evolved hydrogen were recorded as a function of electrolysis time (t = 0 to 20 minutes). The steady state is usually reached after between 10 and 20 minutes of electrolysis.

The polarization curves as a function of current density, U_{cell} = f(j), taken when the steady state was reached after 20 minutes of electrolysis at a given current intensity I, are summarized in Fig. 16 for the different methanol concentrations and working temperatures. These curves are relatively independent of methanol concentration (except for 0.1 M which is not given in Fig.16), at a given temperature, but the polarization curves depend greatly on the cell temperature for a given methanol concentration. These polarization curves are similar to those encountered in the electrocatalytic oxidation of methanol on a Pt-Ru electrode in a DMFC [50].

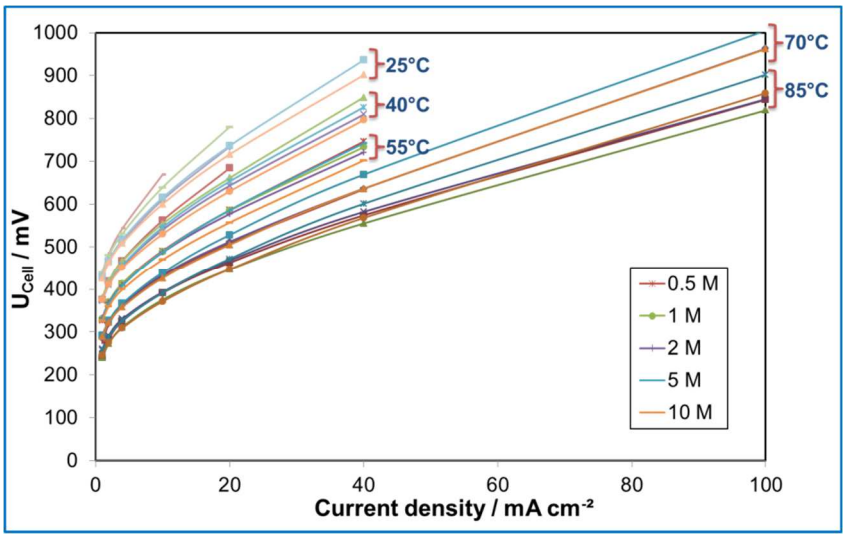

Fig. 16: Polarization curves of methanol oxidation for several methanol concentrations (0.5 to 10 M) and at different working temperatures (25 to 85 °C).

The hydrogen evolution rate was determined by measuring the volume of evolved hydrogen as a function of time at several current intensities (I = 1 to 500 mA) during the electrolysis of different concentrations of methanol (0.5 to 10 M).

In all experiments the measured volume of hydrogen is a linear function of the electrolysis time Δt (Fig. 17(a)) and of the current intensity I (Fig. 17(b)), showing clearly that the volume of evolved hydrogen does not depend on the methanol concentration, nor on the cell temperature, nor on the nature of the anode catalyst, but only on the quantity of electricity involved, $\Delta q = I\,\Delta t$, as a linear function according to equation (13b).The 3 plots in Fig. 17(a), obtained at 50 mA are quite superimposed, in accordance with the Faraday's law.

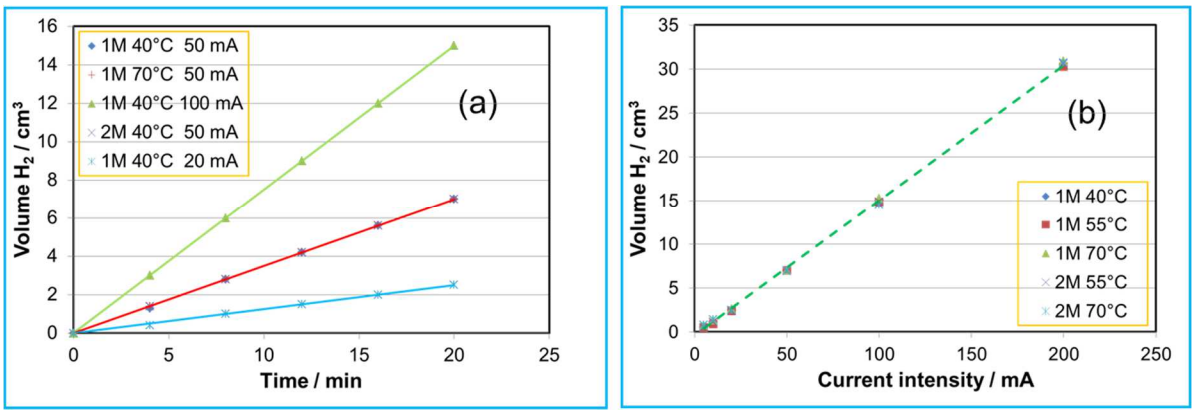

Fig. 17: Examples of curves giving the volume of evolved hydrogen for 2 methanol solutions (1 M and 2 M) as a function of: (a) the electrolysis time Δt at 2 working temperatures (40 and 70 °C) and different current intensities (20, 50 and 100 mA); (b) the current intensity I after 20 minutes of electrolysis at 3 working temperatures (40, 55, 70 °C).

Tables 3 and 4 give the experimental volume of evolved hydrogen, the measured cell voltage U_{cell}, the experimental cell resistance R_{exp}, the cell voltage corrected from ohmic losses and the electrical energy W_e needed to produce one Nm^3 of hydrogen after 20 min. of electrolysis, according to equation (12), as a function of methanol concentration (Table 3) and of cell temperature (Table 4).

Table 3: Experimental volume of generated H_2, cell voltage, interfacial resistance R_{exp}, cell voltage corrected from ohmic losses, and electrical energy W_e, for several methanol concentration after 20 min. electrolysis at 70°C and I = 100 mA with a PtRu(1:1)/C anode.

[MeOH] / mol L^{-1}	Volume of evolved H_2 / cm^3	Cell voltage / mV	R_{exp} / Ω	Corrected cell voltage / mV	W_e / kWh $(Nm^3)^{-1}$
0.1	15.3	651	2.2	431	0.94
0.5	14.6	509	0.89	420	0.92
1	15.3	512	0.93	419	0.92
2	14.5	512	0.95	417	0.91
5	14.6	528	1	428	0.94
10	14.7	505	0.98	407	0.89

As observed in Fig. 17(b) and in Tables 3 and 4, the volume of hydrogen evolved after 20 minutes of electrolysis only depends on the current intensity irrespective of methanol concentration, working temperature, cell voltage, and nature of the anode catalyst. But the electrical energy consumed depends greatly on the working temperature and on the nature of the anode catalyst, since it is related to the cell voltage, i.e. to the electrocatalytic activity of the catalyst.

Table 4: Experimental volume of generated H_2after 20 min. electrolysis (compared to V_{H_2theo} = 15.21 cm^3 at 25 °C and 1 atm.), cell voltage, interfacial resistance R_{exp}, cell voltage corrected from ohmic losses, and electrical energy W_e, as a function of temperature for the electrolysis of 2 M methanol at 100 mA in a 5 cm^2 PEMEC with a PtRu(1:1)/C anode.

T / °C	Volume of evolved H_2 / cm^3	Cell voltage / mV	R_{exp} / Ω	Corrected cell voltage / mV	W_e / kWh $(Nm^3)^{-1}$
25	14.8	734	1.9	544	1.19
40	14.6	643	1.36	507	1.11
55	14.9	577	1.14	463	1.01
70	14.5	512	0.95	417	0.91
85	15.0	468	0.75	393	0.87

In all the results obtained the amount of electrical energy used to produce clean hydrogen by the electrochemical decomposition of methanol is below 1.2 kWh $(Nm^3)^{-1}$, since the corrected cell voltage is below 0.55 V, which is at least 3 to 4 times lower than the energy consumed for water electrolysis.

As an example [63] the energy efficiency coefficient of an electrolysis cell fed with methanol at 70°C working at I = 500 mA and at a corrected cell voltage U_{cell} = 0.488 V leading to an energy loss nF η_{loss} = nF (U_{cell} - U_{rev}) = 6x96.485 (0.488 - 0.016)= 273.2 kJ and a decomposition reaction enthalpy ΔH_{EC} = 129.5 kJ (see Table 2) would be:

$$\varepsilon_{EC} = \frac{\Delta H_{EC}}{\Delta H_{EC} + nF\ \eta_{loss}} = \frac{129.5}{129.5 + 237.2} = 0.321 \approx 32\ \%$$

This energy efficiency coefficient is about one half of that of a water electrolysis cell working at U_{cell} = 1.9 V and at 70°c, i.e. $\varepsilon_{EC}^{H2O} = \frac{1.19}{1.9} \approx 63\ \%$

5. Conclusions

The electrocatalytic oxidation of formic acid and methanol has been the subject of many investigations since nearly fifty years both at the fundamental and application levels. These two compounds can be used either in a Direct Oxidation Fuel Cell to produce electrical energy or in a Proton Exchange Membrane Electrolysis Cell to produce clean hydrogen by their electrochemical reforming. The knowledge of the reaction mechanisms of their oxidation on specific and suitable noble metal catalysts is a key-point since the anodic electrochemical reactions involved in both processes are exactly the same and are activated by the same specific electrocatalysts, e.g. Pd-based catalysts for formic acid and Pt-Ru based catalysts for methanol. The investigation of reaction mechanisms needs to use complementary physical methods such as electrochemical methods (voltammetry, chronoamperometry, etc.) coupled with physicochemical (*in situ* Infrared Reflectance Spectroscopy, Differential Electrochemical Mass Spectroscopy) and analytical methods (*on line* gas or liquid chromatography).

Then Direct Oxidation Fuel Cells are described presenting their advantages and drawbacks. DFAFC has a high theoretical open circuit voltage (OCV = 1.40V) due to its negative standard potential (-0.17 V). With Pd-based catalysts the oxidation of formic acid undergoes the dehydrogenation process leading directly to CO_2, thus avoiding the formation of adsorbed -CO intermediates which poison the catalytic sites. DMFC needs more sophisticated electrocatalysts due to the complexity of the reaction mechanism which involves breaking of the C-H bond in the -CH_3 moiety which may produce the irreversible formation of adsorbed -CO intermediate. Thus the oxidation of adsorbed –CO species needs Pt-based electrocatalysts containing more easily oxidizable metals, e.g. Ru which is particularly active. Both DOFC with optimized anode catalysts reach relatively good performances with power density at 0.5 V of the order of 200 mW cm^{-2} for the DFAFC and 350 mW cm^{-2} for the DMFC, but with similar energy efficiency of about 40 %. These performances are one order of magnitude smaller than those of the hydrogen/oxygen PEMFC giving $P_{max} \approx$ 1 to 2 W cm^{-2} and energy efficiency of around 60 % at a cell voltage of 0.75 V.

On the other hand, the feasibility of the production of clean hydrogen by the electrochemical reforming of formic acid and methanol in a PEMEC has been demonstrated with the following important features:

a) the quantity of hydrogen produced only depends linearly on the quantity of electricity involved, $\Delta q = I\,\Delta t$, i.e. on the electrolysis time Δt and the I, irrespective of the nature of the organic compound, of its concentration, of the electrode potential, of the electrocatalyst nature and structure and of the working temperature.

b) conversely the energy consumption W_e, which is proportional to the cell voltage $U_{cell}(I)$, depends greatly on the nature of the organic compound and its electrochemical reactivity, on the nature, composition and structure of the electrocatalyst and on the working temperature (electrochemical and thermal activations). The following important points have been underlined:

- the favourable thermodynamic characteristics of the electrochemical decomposition of formic acid and methanol give very low cell voltages under standard conditions, e.g. U^0_{HCOOH} = - 0.17 V and U^0_{MeOH} = 0.016 V, compared to that of water ($U^0_{H_2O}$ = 1.23 V) – see Table 1 in Section 2.1.

- in most cases the electrochemical reforming of these organic compounds inside a PEM electrolyser occurs at cell voltages (U_{cell} < 1 V) i.e. with an electric energy W_e < 2 kWh $(Nm^3H_2)^{-1}$ lower than those of water electrolysis (1.5 V < U_{cell} < 2 V, leading to $W_e \approx$ 4 to 6 kWh $(Nm^3H_2)^{-1}$), allowing to reduce greatly, at least by a factor of 2 to 4, the electrical energy consumed.

- the energy efficiency, ε_{EC}, is of the order of 23% for formic acid and 32 % for methanol, which is about one third to one half of that of water electrolysis ($\varepsilon_{EC} \approx$ 60 to 70 %).

- depending on the organic compound considered the nature, structure and composition of the electrocatalyst is of prime importance to reduce the overpotential of the oxidation reaction and thus to decrease the cell voltage under working conditions, e.g. $Pd_{0.8}Au_{0.2}$/C for formic acid and $Pt_{0.8}Ru_{0.2}$/C for methanol.

- the development of more active and stable electrocatalysts for the electrochemical reforming of organic compounds is required to decrease further the anodic overpotential of the oxidation reaction. The best approach to meet this challenge is to acquire a detailed knowledge of the reaction mechanism, particularly the identification of the rate determining step (rds), the rate of which must be increased through the development of new electrocatalysts.

A final conclusion is that any organic compound will lead to similar results, since the rate of hydrogen evolution only depends on $\tilde{n} = 2$, the average number of Faradays per mole of hydrogen involved in the overall process. Thus the most interesting organic compounds will be those experiencing a lower cell voltage for their electrochemical decomposition and a high yield of hydrogen produced, which requires a right choice of the best efficient electrocatalyst leading to the lowest overpotential at the highest current intensity, i.e. a high activity, and to the most complete oxidation reaction to CO_2 if possible, i.e. a high selectivity, under the working conditions of the electrolysis process.

References

[1] B. Sørensen, Hydrogen and Fuel Cell Emerging Technologies and Applications, Elsevier Academic Press, New York, 2005.

[2] C. Rice, S. Ha, R.I. Masel, P. Waszczuk, A.Wieckowski, T. Barnard, Direct formic acid fuel cells, J Power Sources,111 (2002) 83-89.

[3] J. Jiang, A. Wieckowski, Prospective direct formate fuel cell, Electrochemistry Communications, 18 (2012) 41-43.

[4] H. Zhang, H. Liu (Eds.) Electrocatalysis of Direct Methanol Fuel Cells. Wiley-VCH, Weinheim (2009).

[5] C. Lamy, C. Coutanceau, J.-M. Léger, The Direct Ethanol Fuel Cell: a challenge to convert Bioethanol cleanly into electric energy, in Catalysis for Sustainable Energy Production, P. Barbaro, C. Bianchini (Eds.), Wiley-VCH, Weinheim (2009) Chap.1, pp. 3-46.

[6] C. Lamy, Operation of fuel cells with biomass resources (hydrogen and alcohols), in *Waste gas treatment for resource recovery*, Piet Lens, Christian Kennes, Pierre Le Cloirec and Marc Deshusses (Eds.), IWA Publishing, London 2006, Chap. 21, 360-384.

[7] V. Bambagioni, M. Bevilacqua, C. Bianchini, J. Filippi, A. Lavacchi, A. Marchionni, F. Vizza, P.K. Shen, Self-Sustainable Production of Hydrogen, Chemicals and Energy from Renewable Alcohols by Electrocatalysis, ChemSusChem 3 (2010) 851-855.

[8]W.L. Guo, L. Li, S. Tian, S.L. Liu, Y.P. Wu, Hydrogen production via electrolysis of aqueous formic acid solutions. Int J Hydrogen Energy 36 (2011) 9415-9419.

[9] C. Lamy, A. Devadas, M. Simoes, C. Coutanceau, Clean Hydrogen Production through the Electrocatalytic Oxidation of Formic Acid in a PEM Electrolysis Cell (PEMEC), Electrochim. Acta 60 (2012) 112-120.

[10] S. R. Narayanan, W. Chun, B. Jeffries-Nakamuara, T. I. Valdez, Hydrogen generation by electrolysis of aqueous organic solutions, US Patent 6299744, 2001; US Patent 6368492, 2002; US Patent 6643284 (2001); US Patent 6533919 (2003); US Patent 0226763 (2003); US Patent 7056428 B2 (2006).

[11] Z. Hu, M. Wu, Z. Wei, S. Song, P. K. Shen, Pt-WC/C as a cathode electrocatalyst for hydrogen production by methanol electrolysis, J. Power Sources 166 (2007) 458-461.

[12] C. R. Cloutier, D. P. Wilkinson, Electrolytic production of hydrogen from aqueous acidic methanol solutions. Int J Hydrogen Energy 35 (2010) 3967-3984.

[13] A. Caravaca, F.M. Sapountzi, A. de Lucas-Consuegra, C. Molina-Mora, F. Dorado, J.L. Valverde, Electrochemical reforming of ethanol-water solutions for pure H_2 production in a PEM electrolysis cell, Int. J. Hydrogen Energy 37 (2012) 9504-9513.

[14] C. Lamy, T. Jaubert, S. Baranton, C. Coutanceau, Clean hydrogen generation through the electrocatalytic oxidation of ethanol in a Proton Exchange Membrane Electrolysis Cell (PEMEC). Effect of the nature and structure of the catalytic anode, J. Power Sources 245 (2014) 927-936.

[15] A.T. Marshall, R.G. Haverkamp, Production of hydrogen by the electrochemical reforming of glycerol–water solutions in a PEM electrolysis cell. Int. J. Hydrogen Energy 33 (2008) 4649 – 4654.

[16]P. A. Selembo, J. M. Perez, W. A. Lloyd, B. E. Logan, High hydrogen production from glycerol or glucose by electrohydrogenesis using microbial electrolysis cells, Int. J. Hydrogen Energy 34 (2009) 5373-5381.

[17] C. Lamy, Anodic Reactions in Electrocatalysis: Methanol Oxidation. In: G. Kreysa, K.I. Ota, R.F. Savinell (eds.), Encyclopedia of Applied Electrochemistry, Springer Online (2014) pp 85-92.

[18] A. Arico, V. Baglio, V. Antonucci, Direct Methanol Fuel Cells: History, Status and Perspectives. In: H. Zhang, H. Liu (Eds.) Electrocatalysis of Direct Methanol Fuel Cells, Wiley-VCH, Weinheim (2009) Chap 17, pp 1-78.

[19] M. Neurock, M. Janik, A. Wieckowski, A first principles comparison of the mechanism and site requirements for the electrocatalytic oxidation of methanol and formic acid over Pt, Faraday Discussions 140 (2008) 363-378.

[20] C. Lamy, "Electrocatalytic reactions involved in low temperature fuel cells", in "Electrocatalysts for low temperature fuel cells – Fundamentals and Recent trends", T. Maiyalagan and S. Viswanathan (Eds.), Wiley-VCH, Weinheim (2016) Chap.3, pp. 75-111.

[21] C. Lamy, C. Coutanceau, S. Baranton. Production of hydrogen by the electrocatalytic oxidation of low weight compounds (HCOOH, MeOH, EtOH), in “Production of Clean Hydrogen by Electrochemical Reforming of Oxygenated Organic Compounds”,

Hydrogen and Fuel Cells Primers (B. Pollet, Ed.), Elsevier-Academic Press, 1st Edition (2019) Chap.4, pp.1-23.

[22] A. Więckowski, J. Sobkowski, A Jablonski, Adsorption and Oxidation of Formic Acid on Platinized Electrode – Test of Validity of radiometric Method, J. Electroanal. Chem., 55 (1974) 383-389.

[23] J.B. Day, P.A. Vuissoz, E. Oldfield, A. Wieckowski, J.P. Ansermet, Nuclear magnetic resonance spectroscopic study of the electrochemical oxidation product of methanol on platinum black, JACS 118 (1996) 13046-13050.

[24] C. Rice, Y.Y. Tong, E. Oldfield, A. Wieckowski, F. Hahn, F. Gloaguen, J.-M. Léger, C. Lamy, "In Situ" Infrared Study of Carbon Monoxide Adsorbed onto Commercial Fuel-Cell-Grade Carbon-Supported Platinum Nanoparticles: Correlation with ^{13}C NMR Results, J. Phys. Chem. B 104 (2000) 5803-5807.

[25] A. Capon, R. Parsons, The oxidation of formic acid on noble metal electrodes: II. A comparison of the behaviour of pure electrodes, J. Electroanal. Chem. 44 (1973) 239-254.

[26] X. Yu, P. G. Pickup, Recent advances in direct formic acid fuel cells (DFAFC), J. Power Sources 182 (2008) 124–132.

[27] X. Xia, T.J. Iwasita, Influence of Underpotential Deposited Lead upon the Oxidation of HCOOH in $HClO_4$ at Platinum Electrodes, J. Electrochem. Soc. 140 (1993) 2559-2565.

[28] N. Markovic, H. Gasteiger, P. Ross, X. Jian, I. Villegas, M. Weaver, Electro-oxidation mechanisms of methanol and formic acid on Pt-Ru alloy surfaces, Electrochim. Acta 40 (1995) 91-98.

[29] T.D. Jarvi, E.M. Stuve, Fundamental aspects of vacuum and electrocatalytic reactions of methanol and formic acid on platinum surfaces, in: J. Lipkowski, P.N. Ross (Eds.), Wiley, New York (1998).

[30] P.N. Ross, The science of electrocatalysis on bimetallic surfaces, in: J. Lipkowski, P.N. Ross (Eds.), Wiley, New York (1998) p. 63.

[31] G.Q. Lu, A. Crown, A. Wieckowski, Formic Acid Decomposition on Polycrystalline Platinum and Palladized Platinum Electrodes, J. Phys. Chem. B 103 (1999) 9700-9711.

[32] C. Rice, S. Ha, R.I. Masel, A. Wieckowski, Catalysts for direct formic acid fuel cells, J. Power Sources 115 (2003) 229-235.

[33] R. Larsen, S. Ha, J. Zakzeski, R. I. Masel, Unusually active palladium-based catalysts for the electrooxidation of formic acid, J. Power Sources 157 (2006) 78-84.

[34] W. Zhou, J.Y. Lee, Highly active core–shell Au@Pd catalyst for formic acid electrooxidation, Electrochem. Commun. 9 (2007) 1725-1729.

[35] H. Meng, D. Zeng, F. Xie, Recent Development of Pd-Based Electrocatalysts for Proton Exchange Membrane Fuel Cells, Catalysts, 5 (2015) 1221-1274.

[36] G. Zhang, Y. Wang, X. Wang, Y. Chen, Y. Zhou, Y. Tang, L. Lu, J. Bao, T. Lu, Preparation of Pd–Au/C catalysts with different alloying degree and their electrocatalytic performance for formic acid oxidation. Appl. Catal. B: Environ. 102 (2011) 614-619.

[37] A. Papoutsis, J-M. Léger, C. Lamy, New results for the electrosorption of methanol on polycrystalline platinum in acid medium obtained by programmed potential voltammetry, J. Electroanal. Chem., 234 (1987) 315.

[38] E. Herrero, K. Franaszczuk, A. Wieckowski, Electrochemistry of methanol at low index crystal planes of platinum: an integrated voltammetric and chronoamperometric study, J. Phys. Chem., 98 (1994) 5074-5083.

[39] G.-Q. Lu, W. Chrzanowski, A. Wieckowski, Catalytic Methanol Decomposition Pathways on a Platinum Electrode, J. Phys. Chem. B, 104 (2000) 5566-5572.

[40] D. Cao, G.-Q. Lu, A. Wieckowski, S. A. Wasileski, M. Neurock, Mechanisms of Methanol Decomposition on Platinum: A Combined Experimental and ab Initio Approach, J. Phys. Chem. B, 109 (2005) 11622-11633.

[41] B. Beden, A. Bewick, C. Lamy, K. Kunimatsu, Electrosorption of methanol on a Pt-electrode: IR spectroscopic evidence for adsorbed CO species, J. Electroanal. Chem., 121 (1981) 343-347.

[42] C. Coutanceau, F. Hahn, P. Waszczuk, A. Wieckowski, C. Lamy, J.-M. Léger, Radioactive labeling study and FTIR measurements of methanol adsorption and oxidation on fuel cell catalysts, Fuel Cells, 2 (2002) 153.

[43] B. Beden, F. Hahn, C. Lamy, J-M. Léger, N.R. de Taconni, R.O. Lezna, A.J. Arvia, Chemisorption of methanol on different platinum electrodes (smooth and rough polycrystalline, monocrystalline and preferentially oriented) as studied by EMIRS, J. Electroanal. Chem., 261 (1989) 401.

[44] A. Kabbabi, R. Faure, R. Durand, B. Beden, F. Hahn, J.-M. Léger, C. Lamy, In situ FTIRS study of the electrocatalytic oxidation of carbon monoxide and methanol at platinum-ruthenium bulk alloy electrodes, J. Electroanal. Chem. 444 (1998) 41-53.

[45] P. Waszczuk, A. Wieckowski, P. Zelenay, S. Gottesfeld, C. Coutanceau, J.-M. Léger, C. Lamy, Adsorption of CO poison on fuel cell nanoparticle electrodes from methanol solutions: a radioactive labelling study, J. Electroanal. Chem. 511 (2001) 55.

[46] E.M. Be1gsir, H. Huser, J.-M. Léger, C. Lamy, A kinetic analysis of the oxidation of methanol at platinum-based electrodes by quantitative determination of the reaction products using liquid chromatography, J. Electroanal. Chem. 225 (1987) 281-286.

[47] N.H. Li, S.G. Sun, S.P. Chen, Studies on the role of oxidation states of the platinum surface in electrocatalytic oxidation of small primary alcohols, J. Electroanal. Chem. 430 (1997) 57-67.

[48] B. Beden, F. Kadirgan, C. Lamy, J-M. Léger, Electrocatalytic oxidation of methanol on platinum based binary electrodes, J. Electroanal. Chem., 127 (1981) 75-85.

[49] C. Lamy, J.M. Léger, Advanced electrode materials for the Direct Methanol Fuel Cell, in "Interfacial Electrochemistry. Theory, Experiment and Applications", A. Wieckowski (Ed.), Marcel Dekker, New York, chap. 48 (1999) pp. 885-894.

[50] A. Lima, C. Coutanceau, J.-M. Léger, C. Lamy, Investigation of ternary catalysts for methanol electrooxidation, J. Appl. Electrochem., 31 (2001) 379-386.

[51] P. Waszczuk, J. Solla-Gullon, H.-S. Kim, Y. Y. Tong,V. Montiel, A. Aldaz, A. Wieckowski, Methanol Electrooxidation on Platinum/Ruthenium Nanoparticle Catalysts, J. Catalysis, 203 (2001) 1–6.

[52] P. Waszczuk, G.-Q. Lu, A. Wieckowski, C. Lu, C. Rice, R.I. Masel, UHV and electrochemical studies of CO and methanol adsorbed at platinum/ruthenium surfaces, and reference to fuel cell catalysis, Electrochim. Acta 47 (2002) 3637-3652.

[53] L. Dubau, C. Coutanceau, E. Garnier, J.-M. Léger, C. Lamy, Electrooxidation of methanol at platinum-ruthenium catalysts prepared from colloidal precursors: Atomic composition and temperature effects, J. Appl. Electrochem., 33 (2003) 419-429.

[54] M. Watanabe, S. Motoo, Electrocatalysis by ad-atoms. 2. Enhancement of oxidation of methanol on platinum by ruthenium ad-atoms, J. Electroanal. Chem. 60 (1975) 267-283.

[55} D.M. Fadzillah, S.K. Kamarudin, M.A. Zainoodin, M.S. Masdar, Critical challenges in the system development of direct alcohol fuel cells as portable power supplies: An overview, Int. J. Hydrogen Energy 44 (2019) 3031-3054.

[56] B.C. Ong, S.K. Kamarudin, S. Basri, Direct liquid fuel cells: A review, Int. J. Hydrogen Energy 42 (2017) 10142-10157.

[57] Y.W. Rhee, S.Y. Ha, R.I. Masel, Crossover of formic acid through Nafion® membranes, J. Power Sources 117 (2003) 35-38.

[58] X. Wang, J.M. Hu, I.M. Hsing, Electrochemical investigation of formic acid electro-oxidation and its crossover through a Nafion®membrane, J. Electroanal. Chem., 562 (2004) 73-80.

[59] C. Lamy, J.-M. Léger, S. Srinivasan, Direct Methanol Fuel Cells: From a Twentieth Century Electrochemist's Dream to a Twenty-first Century Emerging Technology, in Modern Aspects of Electrochemistry, J. O'M. Bockris, B. E. Conway and R. E. White (Eds.), Kluwer Academic / Plenum Publishers, New York, 2001, Vol. 34, Chap.3, pp. 53-118.

[60] A. Hamnett, Direct Methanol Fuel Cells (DMFC) in Handbook of Fuel Cells: Fundamentals and Survey of Systems, W. Vielstich, A. Lamm and H. Gasteiger (Eds.), Wiley, Chichester, 2003, Vol. 1, Chap. 18, pp. 305-322.

[61] L. Gong, Z. Yang, K. Li, W. Xing, C. Liu, J. Ge, Recent development of methanol electrooxidation catalysts for direct methanol fuel cell, J. Energy Chem. 27 (2018) 1618–1628.

[62] C. Coutanceau, A.F. Rakotondrainibe, A. Lima, E. Garnier, S. Pronier, J.-M. Léger, C. Lamy, Preparation of Pt-Ru bimetallic anodes by galvanostatic pulse electrodeposition: characterization and application to the direct methanol fuel cell, J. Appl. Electrochem., 34(2004) 61-66.

[63] B. Guenot, M. Cretin, C. Lamy, Clean Hydrogen Generation from the Electrocatalytic Oxidation of Methanol inside a Proton Exchange Membrane Electrolysis Cell (PEMEC): effect of methanol concentration and working temperature, J Appl. Electrochem 45 (2015) 973–981.

[64] C. Lamy, P. Millet, A critical review on the definitions used to calculate the energy efficiency coefficients of water electrolysis cells working under near ambient temperature conditions, J Power Sources 447 (2020) 227350.

[65] T. Take, K. Tsurutani, M. Umeda, Hydrogen production by methanol–water solution electrolysis. J Power Sources 164 (2007) 9–16.

[66] G. Sasikumar, A. Muthumeenal, S.S. Pethaiah, N. Nachiappan, R. Balaji, Aqueous methanol electrolysis using proton conducting membrane for hydrogen production, Int. J. Hydrogen Energy 33 (2008) 5905-5910.

[67] S. Uhm, H. Jeon, T. J. Kim, J. Lee. Clean hydrogen production from methanol–water solutions via power saved electrolytic reforming process, J Power Sources 198 (2012) 218–222.

[68] F.M. Sapountzi, M.N. Tsampas, H.O.A. Fredriksson, J.M. Gracia, J.W. Niemantsverdriet, Hydrogen from electrochemical reforming of C1-C3 alcohols using proton conducting membranes, Int. J. Hydrogen Energy 42 (2017) 10762-10774.

[69] J.C. Amphlett, K.A.M. Creber, J.M. Davis, R.F. Mann, B.A. Peppley, D.M. Stokes, Hydrogen production by steam reforming of methanol for polymer electrolyte fuel cells, Int J Hydrogen Energy 19 (1994) 131–137.

[70] S. Sá, H. Silva, L. Brandão, J.M. Sousa, A. Mendes, Catalysts for methanol steam reforming-A review. Applied Catal B Environmental 99 (2010) 43–57.
[71] L. Dubau, F. Hahn, C. Coutanceau, J.-M. Léger, C. Lamy, On the structure effects of bimetallic PtRu electrocatalysts towards methanol oxidation, J. Electroanal. Chem., 554 (2003) 407-415.

Figure captions

Fig.1: Schemes of a Direct Oxidation Fuel Cell (DOFC) (a) and of a Proton Exchange Membrane Electrolysis Cell (PEMEC) (b) using an oxygenated organic compound.

Fig.2: Theoretical electrical characteristics $j(E)$ for a reaction kinetics controlled by the Butler-Volmer law ($\alpha = 0.5$, $n = 2$): $C_xH_yO_z$ oxidation, H_2O oxidation, O_2 reduction and proton reduction. $U_{C_xH_yO_z}$, U_{H_2O}, E_{DOFC} and E_{H_2FC} are the cell voltages for $C_xH_yO_z$ electrolysis, water electrolysis, direct oxidation fuel cell and hydrogen/oxygen fuel cell at a given current density j, e.g. 1 A cm^{-2}.

Fig. 3: Voltammetric curves recorded during the oxidation of 10^{-2} M HCOOH in 0.5 M H_2SO_4 N_2-purged electrolyte on (a) different Pd_xAu_{1-x}/C catalysts and (b) different Pd_xPt_{1-x}/C and $Pd_{0.8}Au_{0.2}$/C catalysts (T = 25 °C ; v = 50 mV s^{-1}). After [9].

Fig.4: Current vs. potential curves for the oxidation of 0.1 M methanol in 0.5 M H_2SO_4on Pt-Ru/C electrodes as a function of their atomic composition (room temperature). After [53].

Fig.5: Cell voltage (A) and power density (B) vs. current density plots of formic acid oxidation with a Membrane Electrode Assembly (MEA) consisting of a Nafion®117 membrane coated with unsupported platinum black (Johnson Matthey, 7 mg/cm^2 at the cathode and 4 mg/cm^2 at the anode) for different HCOOH concentrations at 60 °C. After [2].

Fig.6: Plot of the current density at a 0.4 V cell voltage vs. formic acid concentration. Cell temperature 60°C; formic acid flow rate 1 ml/min. Humidified (70°C) O_2 supplied at a flow rate of 100 sccm. After [2].

Fig. 7: Cell voltage vs. current density curves on a per membrane surface area basis (A) and a per total catalyst weight basis (B) of a direct formic acid fuel cell with various Pd anode catalysts operating in dry air at 30°C with 5 M HCOOH. After [33].

Fig. 8: Power density vs. current density plots on a per membrane surface area basis (A) and a per total catalyst weight basis (B) of a direct formic acid fuel cell with various Pd anode catalysts operating in dry air at 30°C with 5 M formic acid. After [33].

Fig. 9: Schematic diagram of a DMFC based on a Proton Exchange Membrane.

Fig. 10: $E(j)$ and $P(j)$ curves of a single DMFC with Pt-Ru/C electrodes of different Pt-Ru atomic ratios. Anode loading: 2 mg cm^{-2} Pt-Ru / C; Membrane: Nafion® 117; Cathode loading: 2 mg cm^{-2} Pt / C; [MeOH] = 2 M, 2 mL min^{-1}, p_{MeOH} = 2 bar; T_{cell} = 110°C; O_2 = 120 mL min^{-1}, p_{O2} = 2.5 bar ; $T_{MeOH} = T_{O2}$ = 95°C. After Ref. [62].

Fig 11: Electrolysis cell voltage U_{cell} (a) vs. electrolysis time at different current density j - (♦) j = 40 mA cm^{-2}, (■) j = 80 mA cm^{-2}, (▲) j = 120 mA cm^{-2}, (●) j = 160 mA cm^{-2} - and (b) vs. current density after 30 min electrolysis for the oxidation at 25°C of (2 M, 5 M and 10 M) formic acid in a PEMEC (0.5 M H_2SO_4, Pt/C, N117, $Pd_{0.8}Au_{0.2}$/C).

Fig. 12: Hydrogen evolution vs. electrolysis time at several current densities for the PEMEC (0.5 M H_2SO_4, Pt/C, N117, $Pd_{0.8}Au_{0.2}$/C, x M HCOOH) at 25 °C. (♦) j = 40 mA cm^{-2}, (■) j = 80 mA cm^{-2}, (▲) j = 120 mA cm^{-2}, (●) j = 160 mA cm^{-2}, (■) j = 200 mA cm^{-2}.

Fig. 13: Hydrogen evolution at 25 °C as a function of the current intensity for the PEMEC with different anode catalyst (0.5 M H_2SO_4, Pt/C, N117, Pd_xM_{1-x}/C) and several HCOOH concentrations (2 to 10 M). (■) $Pd_{0.8}Au_{0.2}$/C, (▲) $Pd_{0.8}Pt_{0.2}$/C, (◆) $Pd_{0.9}Au_{0.1}$/C.

Fig. 14: CO stripping voltammograms (25°C, 10 mV s^{-1}, 0.1 M $HClO_4$) of the supported catalysts: Pt/XC72 (.—.); Pt-Ru(80:20)/XC72 (.▬.); Pt+Ru(80:20)/XC72 (.▬.); Pt/XC72+Ru/XC72 (.▬.); CO adsorption from (a) a CO saturated solution at 0.1 V for 3 min.; (b) a 0.1 M methanol solution. After [71].

Fig. 15: Quasi-stationary polarization curves recorded at 1 mV s^{-1} and at several temperatures (from 25°C to 85 °C) for the oxidation of 1 M methanol in 0.5 M H_2SO_4 in a DMFC of 5 cm^2 surface area electrodes with a PtRu(1:1)/C anode (4 mg cm^{-2}).

Fig. 16: Polarization curves of methanol oxidation for several methanol concentrations (0.5 to 10 M) and at different working temperatures (25 to 85 °C).

Fig. 17: Examples of curves giving the volume of evolved hydrogen for 2 methanol solutions (1 M and 2 M) as a function of: (a) the electrolysis time Δt at 2 working temperatures (40 and 70 °C) and different current intensities (20, 50 and 100 mA); (b) the current intensity I after 20 minutes of electrolysis at 3 working temperatures (40, 55, 70 °C).

List of Tables

Table 1: Standard thermodynamic data, cell voltage and number of hydrogen moles, N_{H2}, produced by the electrochemical reforming of different hydrogen containing compounds.

Table 2: Summary of the results obtained for $Pd_{0.8}Au_{0.2}$/C at 25 °C with [HCOOH] = 5 M; U_{cell} is the PEMEC voltage and W_e is the electrical energy.

Table 3: Experimental volume of generated H_2, cell voltage, interfacial resistance R_{exp}, cell voltage corrected from ohmic losses, and electrical energy W_e, for several methanol concentration after 20 min. electrolysis at 70°C and I = 100 mA with a PtRu(1:1)/C anode.

Table 4: Experimental volume of generated H_2 after 20 min. electrolysis (compared to V_{H_2theo} = 15.21 cm^3 at 25 °C and 1 atm.), cell voltage, interfacial resistance R_{exp}, cell voltage corrected from ohmic losses, and electrical energy W_e, as a function of temperature for the electrolysis of 2 M methanol at 100 mA in a 5 cm^2 PEMEC with a PtRu(1:1)/C anode.